GNGTS 2024

DISASTER RISK ANALYSIS AND REDUCTION

Session 2.1

Towards new approaches to estimate earthquake and tsunami hazard: a discussion

Convenors of the session:

Daniela Di Bucci **– daniela.dibucci@protezionecivile.it**
Dario Albarello **– dario.albarello@unisi.it**
Bruno Pace **– bruno.pace@unich.it**

The workshop

Approaches for the evaluation of seismic hazard models in Italy

The session will host a workshop on "Approaches for the evaluation of seismic hazard models in Italy", which takes up and develops a previous event held Anacapri in September 2023 (https://www.reluis.it/it/divulgazione/eventi/266-workshop-approcci-per-la-valutazione-dei-modelli-di-pericolosita-sismica-in-italia.html).

The workshop aims at addressing issues related to the scientific and technical/applicative assessment of the various seismic hazard models that co-exist in various countries around the world (including Italy). They sometimes lead to the development of seismic hazard analyses whose results may differ in a way that is perceived as relevant.

The workshop will include contributions from eight invited speakers, followed by a general discussion.

Discussion on long term PSHA – a workshop

Daniela Di Bucci, Dario Albarello, Bruno Pace

Within the 2024 GNGTS Conference, Session "Towards new approaches to estimate earthquake and tsunami hazard: a discussion", a workshop has been organised, which aims at addressing issues related to the scientific and technical/applicative assessment of the various seismic hazard models that co-exist in various countries around the world, including Italy. They sometimes lead to the development of seismic hazard analyses whose results may differ in a way that is perceived as relevant.

The workshop takes up and develops a previous event held Anacapri in September 2023 (https://www.reluis.it/it/divulgazione/eventi/266-workshop-approcci-per-la-valutazione-dei-modelli-di-pericolosita-sismica-in-italia.html) and includes contributes from eight invited speakers, followed by a general discussion.

The focus is on long-term hazard in the Italian framework, at the national scale, in the Cornell-McGuire context, with a perspective on open problems that have not yet found a solution. This general theme has various possible areas of application in the background.

Italy represents a unicum with respect to the availability of input data, seismological, geological and historical data; are they all used, and at their best, in seismic hazard models? Is there scope for improving models by considering unused or underused input data?

The topic of uncertainties is developed in its different aspects: where do they lie with respect to the input data, where with respect to the modelling, how can they be correctly taken into account?

And, finally, what consequences the differences between the hazard models considered (different models, updating of existing models, etc.) have in the various fields of application is addressed.

In other words, what do we intend to do in this workshop?

- Discuss the topic of assessing seismic hazard models, in relation to both their scientific value and their practical use.
- Discuss the evolution of seismic hazard models over the last decades (including the role/development of uncertainties) and the consequences of this evolution on their use and on risk models.
- Identify proposals, possible solutions or aspects still to be explored

And what we do NOT intend to do in this workshop?

- Discuss specifically one or the other of the models produced, except for the purpose of exemplification within the more general topics
- Discuss the role of scientific commissions that play roles in seismic hazard studies
- Go into the decision-making processes of the actors using seismic hazard models

The applications of seismic hazard assessments in civil society and the impact of its variations

Mauro Dolce

Interuniversity Consortium ReLUIS

Whenever the results of seismic hazard analyses that enter into the decision-making processes of civil society (design, planning, etc.) have variations compared to previous ones, a great impact can be determined from different points of view. For example, due to the typical timing of the construction process of structures and infrastructures, new constructions or retrofitting interventions are designed for hazard values different from those of the models subsequently obtained and therefore, may be considered inadequate or excessively precautionary even before being built. This could imply a redesign and a further lengthening of construction times, or even retrofit immediately after their realisation. On the other hand, variations in hazard for models developed at different times can disorient people who are less experienced in probabilistic analysis of seismic hazard, causing a possible loss of confidence in the hazard assessments themselves.

In order to encourage discussion and exchange of ideas, the proposed speech identifies and describes, without claiming to be exhaustive, the areas of application of seismic hazard assessments and the implications of variations in the officially adopted hazard models. In particular, the following areas will be considered:

- Technical Standards for Construction (design of new buildings, safety assessment and risk classification of individual existing buildings, design of seismic retrofit
- Seismic classification of territories (eligibility of areas for incentives aimed at the reduction of the risk of individual buildings or areas on which to carry out structural and non-structural prevention actions - microzonation/territorial planning)
- Risk assessments at national and sub-national level (distribution of funds for seismic risk reduction, emergency planning)
- Risk communication (risk awareness of citizens and local administrators)
- Legal and judicial aspects (hindsight bias, according to which the varied hazard had to direct prevention interventions even before its official adoption)

The non-negligibility of the impact of hazard variations requires that particular attention be paid to the management of the use, in the various fields, of the scientific models that may be developed, taking into account the current state of knowledge, the considerable uncertainties in the knowledge of the fundamental parameters and the divergences of approach in the scientific community.

Uncertainty in source parameters and seismic hazard estimation

Stefano Parolai

Department of Mathematics, Informatics and Geosciences, University of Trieste, Via E. Weiss 2, 34128 Trieste, Italy

Seismic hazard assessment requires as a key ingredient a definition of earthquake magnitude both when using a probabilistic approach and through scenario calculations.

The estimation of the size of an earthquake event, represented by the magnitude, in fact makes it possible to calculate the level of ground shaking expected at a certain distance from the rupture (or epicenter, or hypocenter, depending on the metric used), and to calibrate the probability of occurrence of events of different magnitudes in a certain time period and in a certain space.

Over the years, thanks in part to the gradual introduction of new instruments, the development of seismic networks and the refinement of techniques for analyzing recorded data, different magnitude scales have gradually been proposed. For the same event, the magnitude estimates obtained may differ, being made on different frequency bands (period), of the recorded seismic signal, thus related to different processes of the seismic source.

Magnitude is also used to estimate, through empirical relationships, seismic energy. Moment magnitude (Mw), introduced to obviate the saturation problem that affected previous magnitudes (e.g., Ms, mb, Ml, Md), is determined using the long period (low frequency) amplitudes of the source Fourier spectra, controlled by the average dislocation on the rupture. However, these spectral periods are little affected by changes in the stress drop that determines the radiated energy in high-frequency seismic waves, which is extremely relevant to seismic action on a wide range of structures.

In this presentation, a brief review of some of the magnitude scales discussed above and their differences with a view to engineering applications will be proposed. The scales generally used for seismic hazard assessment and mainly now based on low-frequency spectral ordinates, scale reasonably well, at least within the Italian territory. In fact, the well-known saturation effects, for example for Magnitude Ms, occur only at values close to those of historically known maximum magnitudes. The reasonable scaling persists even when considering the level of uncertainty in magnitude estimation due to the limited observations and the observed shaking variations caused by propagation in the heterogeneous crust. However, this uncertainty must be taken into account for an appropriate treatment of this parameter. Finally, the effects that, due to the limitation of existing scales in capturing source processes, contribute to 'aleatoric uncertainty in ground shaking models will be illustrated.

The use of historical and geological data in seismic hazard assessment: available data, modeling opportunities, and uncertainties involved

Gianluca Valensise

INGV, Rome, Italy

Italy features what is probably the longest and most accurate earthquake record of the planet, plus one of the few compilations of seismogenic sources available worldwide. Not only these data are available to everyone, as they were collected by government agencies with the financial contribution of Italy's Department for Civil Protection; they are also stored in effective GIS-based databases, which makes it easy to explore them and extract the information needed by seismic hazard assessment (SHA) practitioners. Nevertheless, they are not error-free, and their uncertainties may reverberate on the quality of SHA at all scales.

Italian historical earthquake data are subject to uncertainties that concern the observed intensities and hence the focal parameters derived from them, or the ability to separate individual events within complex earthquake sequences – a common occurrence for over 50% of the country's earthquakes. Although there exist data documenting earthquakes that occurred in the Middle Ages, the record is well populated – i.e., complete – for only a few centuries back, depending on geographic regions and on their recording history; as the characteristic recurrence interval of most Italian quakes is in the order of a millennium, we are likely to have no record of the activity of many prospective seismogenic sources, which makes it hard to achieve the necessary completeness.

In their turn, Italian seismogenic sources are known to be hard to find and investigate; most of them are very deep or blind, some lie offshore. The country's geology is especially deceitful, as older faults are systematically more evident than their active and seismogenic counterparts, and there are very few cases of documented historical surface faulting. Also in this case, achieving completeness is definitely hard.

In addition to the mere identification of a large earthquake of the past, or of a large potential seismogenic fault, the potential inaccuracies of the historical and geological-tectonic records extend to the elaborations derived from them. Examples

include the assumption of a recurrence model, usually the same for all geographic areas and for all magnitude intervals; the subsequent derivation of a magnitude-frequency distribution, that sometimes contrasts with the evidence supplied by the earthquake record itself; the idea that all large active faults are fully coupled, and hence 100% seismogenic. These conditions should be sorted out beforehand by fostering the interaction of all scientists involved, so as to avoid turning the richness and uniqueness of the Italian historical and geological records into a limitation, rather than an advantage.

Historical and geological-tectonic data are inherently independent epistemically, and could hence support any seismicity model despite their respective incompleteness: but so far this circumstance has not been exploited to the fullest possible extent. I will briefly present examples of all these conditions, and illustrate how to get the best possible information from the multiplicity of data we already have, and where to go to find new supporting information.

Corresponding author: gianluca.valensise@ingv.it

Causes and ways for modelling complexity in fault-based seismic hazard studies

Bruno Pace

Dipartimento di Ingegneria e Geologia, Università di Chieti-Pescara, Chieti, Italy

Probabilistic fault-based and time-dependent seismic hazard studies are commonly used to forecast the time between consecutive earthquakes; however, the fault segmentation model and the slip rate variability over time are critical for obtaining accurate results. Complex coseismic ruptures observed in the last ~15 years (e.g., 2010 Mw 7.1 Canterbury NZ, 2012 Mw 8.6 Sumatra, 2016 Mw 7.8 Kaikōura NZ, 2016 Mw 6.5 central Italy, 2023 Mw 7.8 Turkey-Syria) have shown the need to consider different possible combinations of rupture scenarios. Moreover, geological and paleoseismological observations confirm the slip rate variability, but rarely seismic hazard models consider it. A possible explanation is the presence of networks of active faults, which interact in a complex manner. We present the results of some studies we have done on these topics. In terms of fault segmentation relaxation, we compare different methodologies to obtain fault-based seismic hazard estimates using several rupture scenarios combinations. In term of fault interaction, we show the importance considering the time-dependent viscoelastic relaxation of the lower crust and upper mantle as a possible additional source of stress changes at a regional scale to explain the concatenation of moderate-to-strong earthquakes. In addition to the development of realistic fault models (comprising detailed fault traces and geologic data to constrain surface and sub-surface fault geometry) and the collection of field observations (to constrain long-term slip rates), slip rate variability over time appears as another key parameter that needs to be considered in future fault-based seismic hazard models, given that both coseismic and postseismic processes are possible explanations of the observation. Finally, we suggest a way to better organize the fault data for a new generation of fault-based PSHA, with a transparent methodology to account for the best geological information available in a given region for seismic hazard and risk studies. The proposed approach empowers end-users and decision-makers to identify main fault and fault sections that participate the most to the seismic risk of a site.

Site-specific checks of probabilistic seismic hazard models with macroseismic historical records

Roberto Paolucci

Dipartimento di Ingegneria Civile e Ambientale, Politecnico di Milano, Milano, Italy

Abstract: Probabilistic Seismic Hazard Assessment (PSHA) provides estimates of annual probability of exceedance of ground motion amplitude at a site. Validation or falsification of PSHA results from ground motion records suffer of two main limitations: (i) since a sufficiently large amount of data should be collected at that specific site to make statistical analysis meaningful, checks cannot be carried out at the site scale, but by integrating records from a more or less large portion of the territory where the PSHA is carried out and (ii) the time interval is not sufficiently extended to cover those that are of relevance for the PSHA applications. In a nutshell, testing with ground motion records the PSHA result at a specific site (say, the town of Florence) is not presently feasible, unless very short return periods are considered that are of no relevance from the practical viewpoint. A different perspective comes if, instead or in addition to ground motion records, use is made of the macroseismic historical records. If reference is made to the Italian context, likely representing that of several European countries, completeness of the catalogue of locally observed macroseismic effects (including lack of effects)) during past earthquakes at many historical sites in terms of moderate-to-large values of macroseismic intensity may extend back to at least several centuries. While several researchers argue that correlations between ground motion and macroseismic intensity may be relatively poor, so to prevent the use of the latter one for PSHA testing, such lack of correlation occurs also because the ground motion amplitude recorded at a given site may not be in itself representative of that of a wider urban area, as, instead, is the case of the macroseismic intensity. With no ambition to introduce novel advanced approaches, in this contribution we will present criteria and application examples with reference to a consistency check, with macroseismic historical records, of the hazard estimates at several Italian towns from two seismic hazard models.

Some thoughts on the testing phase of seismic hazard models

W. Marzocchi

University of Naples Federico II

The intrinsic scientific nature of any probabilistic seismic hazard analysis (PSHA) – including national seismic hazard model (NSHM) – implies that its credibility has to be based (only) on a rigorous and extensive testing phase. However, this phase presents many challenges of different nature and limitations. Here we discuss in detail and with some real examples some of the most important ones.

The long-term time scale of NSHM (50 years) limits the possibility to *validate* a model, i.e., to check if NSHM describes satisfactorily independent data that were never used to build the model. However, past observations can be used to check the *consistency* of NSHM, i.e., if the model is able to explain the past observations. The difference between validation and consistency is not only semantic, because building and testing a model with the same past data can easily lead to overfitting, which may boost improperly the credibility of a model; conversely, overfitting is ruled out when testing model with independent data (validation). Being the consistency tests much more common, it must be kept in mind that the outcomes of this testing phase may not reflect the real goodness of a model, because of the unavoidable and often unquantifiable overfit.

Owing to the limited number of recorded ground shaking observations, the consistency of NSHM is also checked by analysing partial outcomes of the model, which may have more data available for testing (the number of data is linked to the power of the test). Specifically, a NSHM is a complex model with two major components: an earthquake rupture forecast model (ERFM) and a ground motion model (GMM). Hence, the consistency of NSHM can be also checked analysing its ERFM capability to describe satisfactorily the space-time distribution of the past large earthquakes. It goes without saying that this is a sine qua non condition, i.e., a reliable NSHM model has to be composed by a ERFM that describes satisfactorily the past earthquake occurrences, but the opposite is not true: an ERFM that describes well the past large earthquake occurrences does not necessarily lead to a good NSHM if the GMM is wrong. In essence, testing the consistency of ERFM can rise a red flag on the credibility of a NSHM model, but it cannot guarantee for its reliability.

Too often (and unfortunately), NSHM is still based on declustered earthquake catalogs, mimicking the ground shaking of the so-called mainshocks. However, a physics-based

method to distinguish mainshocks from all other earthquakes is not available (and maybe it does not exist at all), and the ground shaking of earthquakes that have been removed from the declustering technique (e.g., aftershocks) can be very damaging. Nonetheless, as regards the testing phase, to maintain coherency and to avoid the comparison of apples and pears, any consistency test should consider only data associated to the mainshocks selected, e.g., excluding strong ground shaking in some sites that were caused by aftershocks. If we want to consider all earthquakes or ground shaking data in the testing phase, the NSHM has to be corrected for declustering. Different techniques have been already proposed in scientific literature that are used in MPS19 (Meletti et al., 2019) and in the most recent NSHM of the United States (Field et al. 2023) and New Zealand (Gerstenberger et al., 2023).

One of the most remarkable features about NSHM in Italy is the rich database of macroseismic intensities, which are not measured ground shaking data, but they may be used to mimic them. However, such a kind of data may be affected by significant problems that have to be taken into account. Here, we just list some of the most important ones: (i) the large uncertainties in the transition from macroseismic intensity to numerical values of the shaking such as accelerations and speeds, and vice versa; (ii) the uncertainties on the macroseismic intensities of the past are affected by substantial uncertainties due, for example, to the cumulative effect of earthquakes of a seismic sequence and to the type of soil which is not considered in the hazard model (by definition, NSHM refers to a rigid ground); (iii) macroseismic intensity data sometimes depend on the research group estimating them.

Another point worth being mentioned is the fact that a rigorous testing phase must be based on solid statistical techniques. Sometimes, the outcomes of NSHM are analysed using ad hoc techniques whose statistical properties have not been properly investigated, or even based on untenable assumptions. It goes without saying that this attitude cannot lead to any reliable judgement on NSHM.

Last, but not least, almost all consistency tests that have been made so far are based on the mean (or median) hazard model, neglecting de facto the so-called epistemic uncertainty. In other words, two models having the same mean hazard, but a quite different dispersion of the branches of a logic tree (or alternative models) around the central value, are considered the same. It is easy to demonstrate that this attitude leads to asymmetrical conclusions, i.e., if a NSHM passes the test considering only the mean hazard it may be deemed as consistent with the data, but if it does not pass the test, it cannot be considered necessarily inconsistent with the data. In a more formal approach, the proper scientific interpretation of the seismic hazard estimates requires a probabilistic framework that admits epistemic uncertainties on aleatory variables. This is not straightforward because, to subjectivists, all probabilities are epistemic, whereas to frequentists, all probabilities are aleatory. The inadequacy of purely subjectivist and

purely frequentist interpretations of probability is made evident by examining the probabilistic meaning of the mean hazard in these contexts. Here we describe a unified approach (Marzocchi and Jordan, 2017) that may overcome this problem, allowing formal tests of NSHM.

References

Field, E. H., K. R. Milner, A. E. Hatem, P. M. Powers, F. F. Pollitz, A. L. Llenos, Y. Zeng, K. M. Johnson, B. E. Shaw, D. McPhillips, et al. (2023). The USGS 2023 Conterminous U.S. Time-Independent Earthquake Rupture Forecast, Bull. Seismol. Soc. Am., doi: 10.1785/0120230120

Gerstenberger, M. C., S. Bora, B. A. Bradley, C. DiCaprio, A. Kaiser, E. F. Manea, A. Nicol, C. Rollins, M. W. Stirling, K. KS. Thingbaijam, et al. (2023). The 2022 Aotearoa New Zealand National Seismic Hazard Model: Process, Overview, and Results, Bull. Seismol. Soc. Am., doi: 10.1785/0120230182

Marzocchi, W., T.H. Jordan (2017). A unified probabilistic framework for seismic hazard analysis. Bull. Seismol. Soc. Am., 107(6), 2738-2744.

Meletti, C., W. Marzocchi, V. D'Amico, G. Lanzano, L. Luzi, F. Martinelli, B. Pace, A. Rovida, M. Taroni, F. Visini (2021). The new Italian seismic hazard model (MPS19). Ann. Geophys., 64 (1), SE112

Corresponding author: warner.marzocchi@unina.it

How different PSHA is different enough?

I. Iervolino

[1] *Università degli Studi di Napoli Federico II.*

[2] *IUSS – Scuola Universitaria Superiore di Pavia.*

Probabilistic seismic hazard analysis (PSHA) is widely employed worldwide as the rational way to quantify the uncertainty associated to earthquake occurrence and effects. National-scale PSHA has its results typically expressed in the form of maps of ground motion measures intensities that all have the same exceedance return period. Classical PSHA relies on data that continuously increase due to instrumental seismic monitoring, and on models that continuously evolve with the knowledge on each of its many aspects. Therefore, it can happen that different, equally legitimate, hazard maps for the same region can show apparently irreconcilable differences, sparking public debate. This situation is currently ongoing in Italy, where the process of governmental enforcement of a new hazard map is delayed. The discussion is complicated by the fact that the events of interest to hazard assessment are intentionally rare at any of the sites the maps refer to, thus impeding empirical validation at any specific site. The presentation will show the result of two recent studies, which pursue a regional approach, regarding three different authoritative PSHA studies for Italy. The first one entailed formal tests on the output of PSHA against the observed ground shaking exceedance frequencies, obtained from about fifty years of continuous monitoring of seismic activities across the country (Iervolino et al., 2023a). The second compares the areas in which exceedance of PSHA-postulated ground motion intensity threshold is estimated according to ShakeMap for twelve years of instrumental earthquakes, with what expected from the considered PSHA models (Iervolino et al., 2023b). The bulk of analyses reveals that, apparently alternative hazard maps are, in fact, hardly distinguishable in the light of observations and ShakeMap estimations. This perspective, which may be relevant for the current debate, may be strengthened by the fact that recent studies (Baltzopoulos et al., 2023) also show that structural design, for example for reinforced concrete moment-resisting frames, is strictly dominated by seismic actions only in a fraction of the country, owing to the effect of building-code-prescribed minima and design for gravity loads.

References

Baltzopoulos, G., Grella, A., & Iervolino, I; 2023. Some issues in the practical application of risk-targeted ground motions. *Earthquake Engineering & Structural Dynamics*. DOI: 10.1002/eqe.4058

Iervolino, I., Chioccarelli, E., & Cito, P.; 2023a. Testing three seismic hazard models for Italy via multi-site observations. *PLoS one*, *18*(4), e0284909.x.

Iervolino, I., Cito, P., & Vitale A.; 2023b. Territorial exceedance of probabilistic seismic hazard from ShakeMap data. (In review.).

Corresponding author: iunio.iervolino@unina.it

Earthquake sequences and long-term seismic hazard maps: an oximoron?

P. Bazzurro

University School for Superior Studies (IUSS) in Pavia, Pavia, Italy

Seismic hazard maps for regional or national applications have no interest per se. Their importance resides in their critical support to earthquake risk assessment and, if needed, risk mitigation of specific structures or portfolios of structures. The oldest of the many possible applications of seismic hazard maps involves the definition of the ground motion loads to be used for designing new buildings in such a way that they possess the required level of safety or, equivalently, that have sufficiently low chance of becoming unfit for purpose in a given period of time. Another application, and arguably a more challenging one, involves their use at the basis for assessing the risk that existing buildings of different age and structural typology have to become unfit for occupancy or even to be destroyed by earthquakes in a given period of time. For these applications, and others not mentioned above, it is customary to require that these maps provide a long-term stationary view of the seismic hazard. This has been achieved by adopting a mainshock-only view of the earthquake phenomenon, a tenet that underpins essentially every single hazard map developed worldwide. Evidence has shown, however, that in most parts of the world, including Italy, earthquakes occur in sequences and that large damaging earthquakes not preceded or followed by other nearby events closely spaced in time are a rarity rather than the norm. The larger amount of damage that sequences cause when compared to the damage inflicted by the mainshock only has been apparent for a long time and the Central Italy sequence of 2016-17 is only one recent example. Therefore, given that hazard assessment should serve risk calculations and risk estimates are impacted by the occurrence of all damaging earthquakes, regardless of their label, it is clear that future seismic hazard maps should include the contribution of all earthquakes, not just the mainshocks. Several methods have been proposed to include earthquakes “other” than mainshocks in the hazard/risk calculations, some more elegant than others. We will present a method that allows the development of hazard maps that include the occurrence of realistic sequences that (i) are statistically consistent in time and space with those occurred in the region; (ii) include events with magnitude lower than that of the mainshock of the sequence and that may or may not occur along the same rupture of the mainshock. Such a method, if appropriately managed statistically, may yield maps that still reflect a long-term view estimate of the seismic hazard, but heightened if compared to the traditional hazard estimates that accounts only for mainshocks. The underestimation of the traditional seismic hazard due to the consideration of only mainshocks is, of course, more significant in regions where prolific sequences occur more often. From the risk side more refined engineering models that are able to capture damage accumulation in buildings due to multiple shocks are under development. There is no doubt that these maps are the way of the, hopefully, close future

The general session

Outlining the possible scenarios induced by the occurrence of earthquakes and tsunamis in the next future is an essential task of the seismological research. The close connection of these studies with the risk mitigation regulations has stimulated research in this direction but has also conditioned its development. Many studies have remained confined to restricted academic fields and this has progressively dried up part of the scientific debate, even at an international level. We want to stimulate a broader discussion on the topics, also because new and controversial strategies of analysis are appearing in the limelight. The session aims to reopen the debate on these issues of central importance for the research on hazards, also starting from a terminological redefinition of the problem, overcoming the apparent "sclerosis" of the discussion. The final aim is to outline a research path towards new approaches for seismic and tsunami hazards assessments over the next decade, also including a multi-hazard perspective.

In terms of earthquake hazard the following topics are encouraged:

- **Role and uncertainties of short-term seismic hazard models (days/months), both on statistical and deterministic basis, and how to give them a probabilistic form for their integration with medium-term (years) and long-term (tens of years) estimates.**
- **Seismic hazard estimates related to rare events and possible validation models of these estimates.**
- **Role of macroseismic studies and impact of their uncertainties in long-term seismic hazard definition.**
- **Methods of integrating geological and geophysical, surface and subsoil data, for parametric definition of the sources and their uncertainties, within a probabilistic formulation of hazard and event scenarios.**
- **Development of physics-based models of seismic sources and their interaction.**
- **Critical analysis of propagation models to support near-field and long-range ground motion estimates.**
- **Fault displacement hazard analysis, regarding in particular strategic infrastructures, and its possible integration into seismic hazard models.**
- **Systematic integration of local seismic hazard assessments into the regional scale ones.**

In terms of tsunami hazard the following topics are encouraged:

- **Tsunami hazard models for tsunamis generated by earthquakes, also in comparison with international experiences, and the possible integration with a probabilistic approach of other types of data.**

- **Development of event and impact scenarios and their constituent elements.**
- **Advances in knowledge and modelling for tsunami hazard for tsunamis not generated by earthquakes.**

An improved workflow to efficiently compute local seismic probabilistic tsunami analysis (SPTHA): a case study for the harbour of Ravenna, Italy

E. Baglione[1,2], B. Brizuela[2], M. Volpe[2], A. Armigliato[1], F. Zaniboni[1], R. Tonini[2], J. Selva[3]

[1] *Dipartimento di Fisica e Astronomia, Università di Bologna, Italy*
[2] *Istituto Nazionale di Geofisica e Vulcanologia, Italy*
[3] *Università di Napoli Federico II, Napoli, Italy*

Introduction

Tsunamis pose a significant threat to coastal communities worldwide, prompting the development of Probabilistic Tsunami Hazard Analysis (PTHA) to assess the hazard at varying Average Return Periods (ARPs), spanning from hundreds to thousands of years. By integrating data, physical and statistical models, and expert judgments, Probabilistic Tsunami Hazard Assessment (PTHA) provides a structured method for quantifying hazard and associated uncertainties (Grezio et al., 2017; Behrens et al., 2021; Davies et al., 2022). PTHA is increasingly recognized as the established best practice for effectively managing risk assessment and implementing risk mitigation measures (Løvholt et al., 2017; Tonini et al., 2020; Selva et al., 2021).

Offshore PTHA studies excel in characterising hazard across a broad spectrum of earthquake-tsunami sources over extensive spatial scales while quantifying uncertainties stemming from knowledge gaps. However, their primary drawback lies in the limited modelling of tsunami shoaling and inundation, providing restricted insights into local onshore hazard. Recognizing that regional models often lack the resolution to capture specific local characteristics, the development of a local hazard model becomes imperative.

A local model not only offers more accurate and detailed information but also facilitates more effective planning and mitigation strategies. Moreover, a local model proves invaluable for emergency responders and local authorities by enabling prompt and efficient evacuation and response efforts (Rafliana et al., 2022). Taking into account unique local features such as topography and coastal structures, a local model provides insights that may be overlooked in a regional model. This includes identifying vulnerable areas like small harbours or bays, which

might be particularly susceptible to tsunamis but are not easily discernible in broader regional models.

Hence, developing a local hazard model is an essential step in accurately forecasting the potential impact of tsunamis and developing effective mitigation and response strategies. But turning offshore into high-resolution onshore PTHAs, comprehensively capturing inundation hazard and uncertainty, while resolving spatial scales relevant to risk management on the order of 5-10 m, is a challenging task (Lorito et al., 2015; Lynett et al., 2017; Sepúlveda et al., 2019; Volpe et al., 2019; Gibbons et al., 2020; Tonini et al., 2021; Davies et al., 2022).

In this study we introduce an enhanced method for conducting a local Probabilistic Tsunami Hazard Assessment (SPTHA) based on a regional SPTHA without the need of HPC (High Performance Computing) resources (Fig. 1,a).

The method aims to reduce the computational effort required for a local tsunami assessment, updating and simplifying some previous approaches (Lorito et al., 2015, Volpe et al., 2019). The procedure is tested in the region of Catania, Sicily, south of Italy, and applied to the Ravenna harbour, situated in the Northern Adriatic Sea, Italy (Fig. 1,b).

The method

The developed method allows to refine the regional SPTHA by identifying the most significant tsunami sources that impact the local hazard. The resulting procedure simplifies some previous workflows (Lorito et al., 2015, Volpe et al., 2019) for quantifying local SPTHA and represents a useful tool that can be potentially applied wherever there is regional hazard information available, ultimately leading to improved accuracy in the assessment process.

The first and innovative step of our approach involves the application of an “importance” sampling technique that adopts regional hazard disaggregation as weighting information. A source refinement of the scenarios closest to the target is then applied to the new subset, enhancing the characterization of local sources, thereby improving hazard modelling by capturing natural variability (aleatory uncertainty) and reducing epistemic uncertainty. Offshore tsunami simulations are conducted on the retrieved scenarios and the water height profile over a series of points close to the target area; together with the coseismic field information, it represents the feature for a subsequent filtering operation to further reduce the number of high-resolution tsunami simulations required for the local hazard definition.

The workflow of the approach is reported in Fig. 1. and consists of four main steps: source preselection; source refinement; cluster analysis; local hazard quantification.

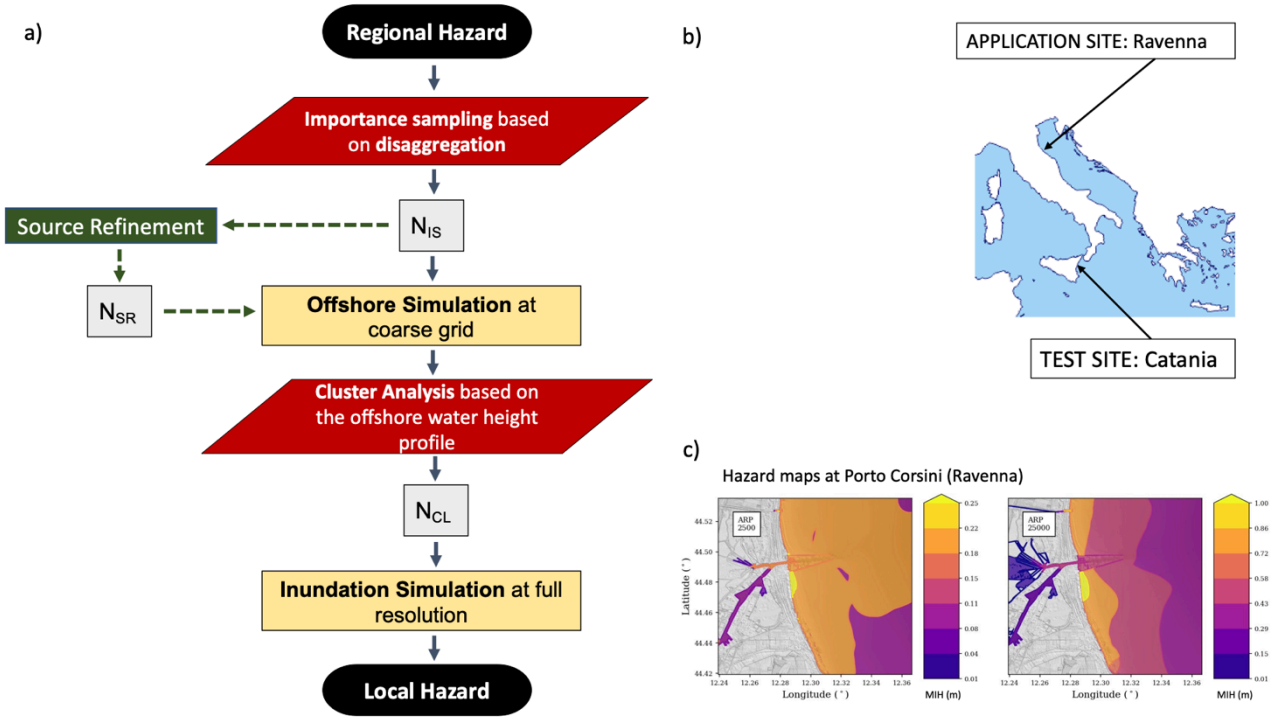

Fig. 1: a) *Schematic diagram of the adopted procedure for evaluating local SPTHA*. b) Spatial representation of Test and Application case sites. c) Hazard maps obtained at the Application site of Ravenna for two different Average Return Periods (ARPs).

Source Preselection

The presence of a Probabilistic Tsunami Hazard Assessment (PTHA) model holds significant importance as it enables the preselection of specific source areas of interest within the region. This capability results in essential time savings during calculations.

At local coastal sites, the offshore PTHA is not able to reproduce the tsunami, as only high-resolution onshore tsunami simulations can guarantee an acceptable level of detail for the description of the local hazard. However, regional PTHA makes a huge effort for homogeneously including all the potential sources of tsunami and for exploring existing aleatory and epistemic uncertainty (Basili et al., 2013, Selva et al., 2016; Davies et al., 2022). This effort allows quantitatively filtering out source areas that do not matter locally, without imposing any subjective qualitative choice.

Source disaggregation offers a quantitative assessment of the potential impact of a particular source area on the local tsunami hazard (Bazzurro and Cornell, 1999; Selva et al., 2016). Specifically, for a designated tsunami intensity threshold, hazard disaggregation provides a measure of the probability that a given source area can produce such an intensity of tsunami.

For a specified target, the regional hazard leads to a nearby point in the regional hazard, with the most representative point for the local target (e.g., the closest point) considered. Disaggregation enables the identification of earthquake scenarios that significantly contribute to the tsunami hazard for the preselected Point of Interest (POI).

The initial operation of our workflow consists of the employment of regional hazard disaggregation as weighting information for an “importance” sampling procedure. This enables sampling in areas of significance, where the likelihood of selecting scenarios that have the most impact on the hazard is higher. By choosing scenarios based on their "importance", this sampling strategy significantly enhances efficiency.

Source Refinement

The combination of importance sampling and hazard disaggregation provides us N_{IS} scenarios that comprehensively capture the total hazard at the most representative point for the target location. Given that the regional hazard is generated with a relatively coarse resolution for both the source and target points, it may be reasonable, at this juncture, to enhance the representation of both the source and target with a more localised perspective (Williamson et al., 2022). This refinement allows for an expanded source discretization, introducing greater variability for the local hazard. If specific local information is accessible, it becomes feasible at this stage to reassign probabilities based on such information, achieving a balanced consideration alongside the regional contribution. This involves perturbing each scenario by sampling alternative values of the source parameters that more accurately characterise it.

Following the refinement of the source, we obtain N_{SR} scenarios (greater than N_{IS}). To maintain the total contribution to the hazard, these new scenarios must undergo reweighting. In the absence of additional information, each new scenario can be assigned to the original scenarios, with equal weight assigned to all scenarios associated with the same original scenario. However, if new local information is accessible (e.g., insights into local fault positions), the weights can vary, with the constraint that they collectively sum to 1 for each original scenario, thus preserving their original balance.

Clustering

The results of offshore simulations serve as input for an additional filtering step before conducting coastal flood simulations on a fine grid. This step involves a cluster analysis of water column height profiles at specific points along a near-shore bathymetric depth, such as at 10 m. These points are strategically distributed in proximity to the site of interest, ensuring an adequate number for the final hazard calculation. It's important to note that without the application of the refinement step, these points might not be adequately resolved from the regional hazard results.

The water height profile, coupled with the vertical coseismic deformation at the corresponding profile location, serves as the proxy variable for the clustering filter (Volpe et al., 2019). For clustering, we employ a standard implementation of K-means clustering (Lloyd, 1982) provided by the Scipy sklearn package (Pedregosa et al., 2011). The selected metric is the Euclidean distance, computed as the square root of the sum of squares of differences in each of the two

proxy variables, and considers both the maximum wave height of the tsunami and the coseismic displacement at each target point. To cluster the N_{SR} original scenarios in proxy-space into N_{CL} clusters, we assign each scenario to the cluster with the closest centroid based on the selected metric.

To assess the convergence of results with an increasing number of clusters, we rely on the Within-Clusters Sum of Squared (WCSS) or inertia provided by the sklearn tool. This enables a quick visualisation of clustering behaviour and facilitates the identification of a suitable minimum number of clusters using the elbow rule. This approach helps determine the minimum clusters necessary for sufficient convergence of results. While larger numbers of clusters may enhance resolution, they come at the expense of increased computational effort.

Following the K-means clustering, a total of N_{CL} clusters are identified. These N_{CL} scenarios serve as a starting point for high-resolution simulations involving flooding at the target site.

For each cluster, we designate a representative scenario as the one whose water height profile deviates the least from the cluster's average. Assuming similar effects on near offshore points, scenarios within the same cluster can be reasonably regarded as inducing comparable inundation. The associated weight for each scenario representative is determined by summing the weights of all scenarios within that cluster. Without refinement, this sum corresponds to the number of scenarios in the cluster. It's worth noting that while K-means clustering is based on water height profiles, scenarios in the same cluster are expected to exhibit a relatively similar profile shape. However, this doesn't guarantee that all scenarios and clusters are equally representative of the final hazard: and that’s why the sum of all within-the-cluster scenarios rates is considered.

Local hazard quantification

High-resolution simulations can be performed for all representative scenarios identified by N_{CL}. The outcomes of these simulations will be utilised to generate hazard curves and maps, offering a representation of our local hazard model. The number of simulations N_{CL} is significantly reduced compared to the number of scenarios making up the initial ensemble: this allows resolution to be carried out even in the absence of a significant computing infrastructure.

The test case

To test the efficiency and validity of the method described, we considered the area of Catania, Sicily, South of Italy. In this test site, numerous numerical simulations have been produced with significant high-performance computing (HPC) resources for recent studies (Gibbons et al., 2020; Tonini et al., 2021). The 32,363 tsunami simulations were conducted through Tsunami-HySEA software over 4 levels of nested grids: one global 0-grid for the open ocean propagation covering the Mediterranean Sea and three local grids (with resolution 160 m, 40 m and 10 m respectively).

Since the available inundation simulations were obtained only for the NEAMTHM18 (Basili et al., 2021) discretization, to not produce further simulation, we skipped the source refinement. The available simulations were sufficient to produce the target point refinement. A set of 8 target points were defined along the 10 m bathymetric line, covering the entire target area (see Fig. 2,a). The results of simulations were retrieved at these new points. The convergence of hazard curves with the N_{IS} was checked also on these points (see Fig. 2,d-g).

Focusing on the results of simulations on these new points, we conducted the cluster analysis for different numbers of clusters N_{CL} (50, 100, 250): Fig. 2,b shows the WCSS applied to the N_{IS} ensemble. For each of these cluster sets we have reproduced the hazard curves (N_{CL}= 250 in Fig. 2,d-g) on the flow depth data on some points of the area of interest and the inundation maps (N_{CL}= 250 in Fig. 3), in order to compare the results obtained with those conducted starting from all the scenarios thanks to the HPC resources. As in Gibbons et al. (2020), no uncertainty is modelled in simulation results and a Heaviside step function is used that is 1 if the intensity computed by NLSW (Non-Linear Shallow Water) simulations for the scenario is greater than the reference MIH (Maximum Inundation Height) value, and 0 otherwise.

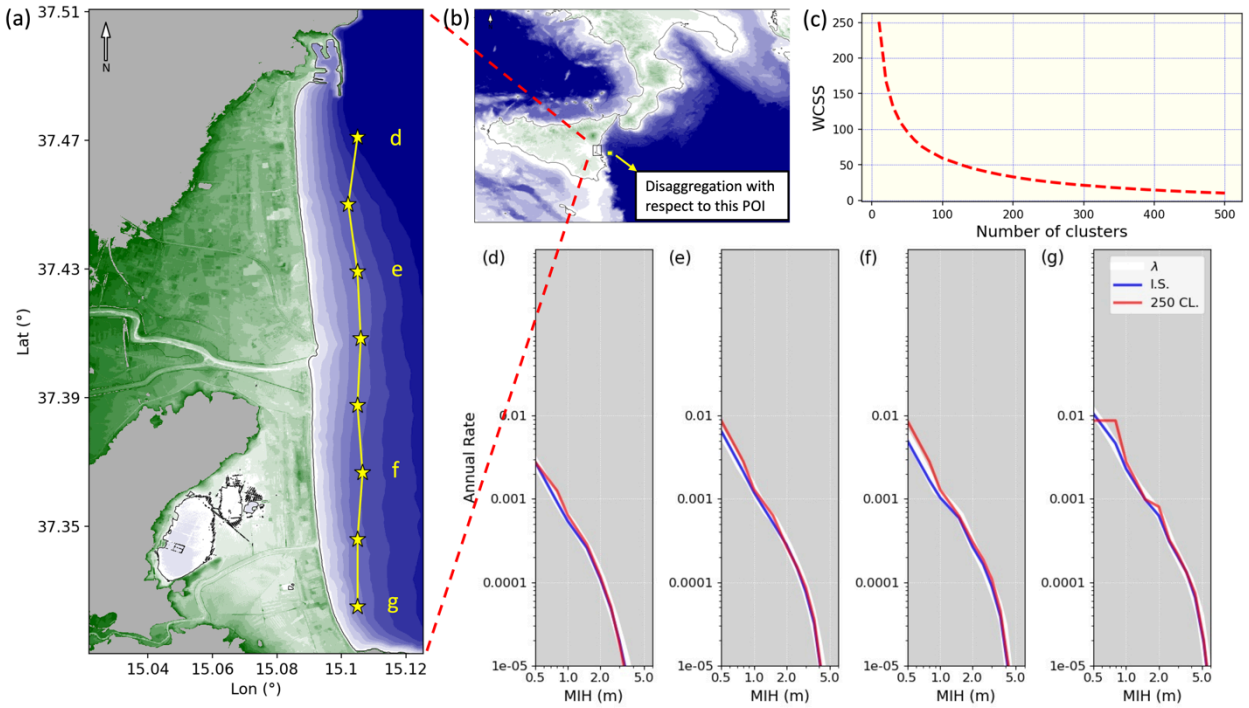

Fig. 2: a) Setup for the cluster analyses in the Catania site. Subplot (a) shows a zoom of the finest grid for the Catania harbour from: in the wider map (b) it is highlighted the location of the target site on the Sicilian Island, with respect to which the disaggregation was conducted. (c) subplot displays the WCSS (Within-Cluster Sum of Squares) behaviour for an increasing number of clusters. (d), (e), (f), (g) subplots are the annual rates evaluated for the total (white curve), importance sampling (blue curve) and cluster (red curve) rates respectively: the plots refer to the same letter locations highlighted in (a) subplot.

Hazard maps (for two different annual return periods) are displayed in Fig. 3: the differences between our results and the HPC ones are very small and nearly negligible for ARP 2500 yrs.

Considering the good results shown in the comparison with the outputs of the HPC implementation, we proceeded to apply the method implemented to the chosen case study.

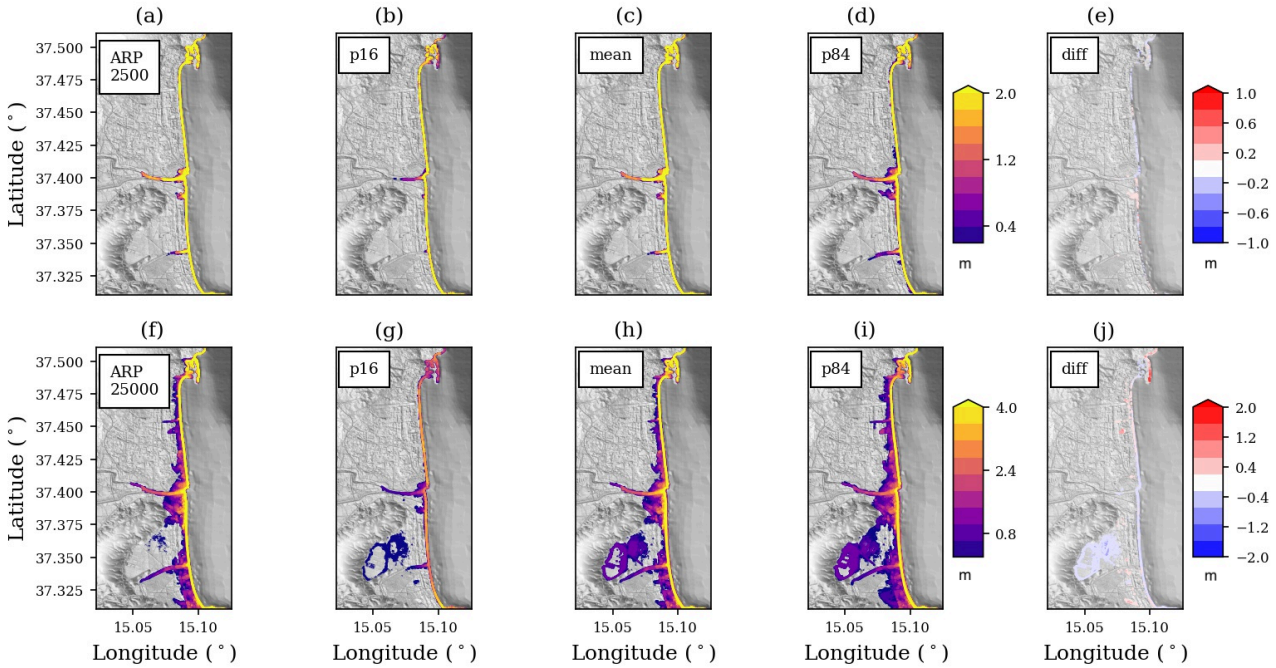

Fig. 3: a) Hazard maps for the flow-depth for different annual return periods. (a) and (d) plots represent our results for the 250 clusters. Plots in (b)-(g), (c)-(h), (d)-(i) represent the 16th percentile, the mean and the 84th percentile of the results obtained with the use of massive HPC. Last two columns (e) and (j) represent the difference between our results in the first columns and the mean values on the (c)-(h) columns.

The application

We applied the method to the North Adriatic region of Ravenna, particularly monitored for the subsidence that characterises the area and its important port. Porto Corsini, along the Adriatic coast, has consistently held a crucial role as a maritime hub (Perini et al., 2017; Armaroli et al., 2019). The port's strategic location has facilitated the efficient transportation of goods, people, and ideas throughout the region and beyond. With its proximity to major international trade routes, Porto Corsini has emerged as a crucial link connecting Italy to the broader global network of maritime commerce.

Studying the tsunami hazard in this area can play a useful perspective to help enabling the identification and implementation of effective mitigation measures to safeguard the port's infrastructure, maritime activities, and the surrounding coastal community from potential catastrophic events, ensuring the uninterrupted functioning of this vital maritime hub.

The bathymetric and topographic grid models for the simulations were built adopting the European Marine Observation and Data Network (EMODnet) project database (EMODnet DTM version released in 2018, http://portal.emodnet-bathymetry.eu/, last access: 23 April 2021), the European Digital Elevation Model (EU-DEM), version 1.1 (eu_dem_v11_E50N10). Superimposed on these grids, for greater detail in the target area, two nautical maps have been digitised. The

computational domain for tsunami propagation consisted of five levels of nested grids with increasing resolution approaching the Ravenna harbour (640, 320, 80, 20 and 5 m, respectively). The tsunami simulations were conducted with the Tsunami-HySEA software. Implemented in CUDA (Compute Unified Device Architecture) and parallelized for running in multi-GPU architectures (de la Asunción et al., 2013), the code solves the non-linear shallow water. It has passed proper benchmarking, in particular the National Tsunami Hazard and Mitigation Program, USA (Macías et al., 2017, 2020b, 2020a).

The method shown in Fig. 1,a diagram has been adopted. In addition to the Catania test case, we applied the source refinement step.

The regional model is again represented by the NEAMTHM18 tsunami hazard model (Selva et al. 2016, Basili et al., 2021). The first massive selection of scenarios involves the application of weighted importance sampling with disaggregation. This operation, carried out with a target near Ravenna, provides a total of about 1500 scenarios of the ensemble composing the regional hazard.

The close sources (within the first 125 km from the target location) are perturbed 10 times around their NEAMTHM18 values. The far sources are not perturbed. This operation widens the number of scenarios (about 4000) and considerably enriches the variability of the source: this can be a welcome operation in the passage from a regional description to a local one.

The obtained scenarios are the input for the first set of tsunami simulations conducted over 4 (6 for the more distant sources) hours of propagation on the first 3 grids of the bathymetrical domain. The water profiles over 7 points of the 80 m resolution grids, taken at an approximated depth of 10 m, are the inputs for the subsequent filtering conducted with a clustering algorithm.

The final set of simulations (on 250 cluster representative scenarios) is run over all the available grids, reaching the higher resolution of 5m in the proximity of the target area, the Ravenna harbour.

The results obtained with the fine grid simulations are used to produce the hazard maps for maximum inundation height (Fig. 1,c). Alongside the hazard results, the behaviour of the waves inside the Porto Corsini canal was studied, in order to retrieve useful information for sites and structures near the canal, taking advantage of the use of detailed bathymetry (5 m resolution).

Conclusion

In this study, we developed a local hazard model based on an existing regional model: this approach significantly reduces the computational workload without sacrificing precision or complexity. The key ingredient to reduce computational load and introduce an innovative strategy is represented by the coupling of the probabilistic insights gained from disaggregation with targeted sampling through importance sampling. This combination allows for an effective selection of scenarios that contribute most to the hazard, without the need for arbitrary and subjective cuts. The resulting ensemble is substantially reduced compared to the initial scenario

count: a refinement procedure is then applied to enhance information from the local source, thereby diminishing associated epistemic uncertainty. This step serves as the foundation for medium-scale simulations, maintaining a balance between comprehensiveness and detailed intricacies.

The offshore profiles of these simulations furnish the input for a subsequent filtering process using a K-means algorithm, which groups scenarios into clusters sharing similar wave shape and amplitude profiles. The representatives of these clusters are then selected for the final phase: conducting high-resolution flood simulations to define hazard curves and maps at the local level.

The method is tested and validated in the port area of Catania, thanks to the comparison with the already available results derived from massive simulations using high-performance computing. The results exhibit a good agreement between the proposed method and the exhaustive use of all scenarios in the ensemble. The new method is further applied to the port of Ravenna, where a high-resolution grid structure has been meticulously established.

References

Armaroli, C., Duo, E., and Viavattene, C. (2019). From Hazard to Consequences: Evaluation of Direct and Indirect Impacts of Flooding Along the Emilia-Romagna Coastline, Italy. *Frontiers in Earth Science* 7. Available at: https://www.frontiersin.org/articles/10.3389/feart.2019.00203 [Accessed June 28, 2023].

Basili, R., Tiberti, M. M., Kastelic, V., Romano, F., Piatanesi, A., Selva, J., et al. (2013). Integrating geologic fault data into tsunami hazard studies. *Natural Hazards and Earth System Sciences* 13, 1025–1050. doi: 10.5194/nhess-13-1025-2013.

Basili, R., Brizuela, B., Herrero, A., Iqbal, S., Lorito, S., Maesano, F. E., et al. (2021). The Making of the NEAM Tsunami Hazard Model 2018 (NEAMTHM18). *Front. Earth Sci.* 8. doi: 10.3389/feart.2020.616594.

Bazzurro, P., & Allin Cornell, C. (1999). Disaggregation of seismic hazard. *Bulletin of the Seismological Society of America*, *89*(2), 501-520.

Behrens, J., Løvholt, F., Jalayer, F., Lorito, S., Salgado-Gálvez, M. A., Sørensen, M., et al. (2021). Probabilistic Tsunami Hazard and Risk Analysis: A Review of Research Gaps. *Frontiers in Earth Science* 9. Available at: https://www.frontiersin.org/articles/10.3389/feart.2021.628772 [Accessed June 28, 2023].

Davies, G., Weber, R., Wilson, K., and Cummins, P. (2022). From offshore to onshore probabilistic tsunami hazard assessment via efficient Monte Carlo sampling. *Geophysical Journal International* 230, 1630–1651. doi: 10.1093/gji/ggac140.

De la Asunción, M., Castro, M. J., Fernández-Nieto, E. D., Mantas, J. M., Acosta, S. O., and González-Vida, J. M. (2013). Efficient GPU implementation of a two waves TVD-WAF method for the two-dimensional one layer shallow water system on structured meshes. *Computers & Fluids* 80, 441–452. doi: 10.1016/j.compfluid.2012.01.012.

Gibbons, S. J., Lorito, S., Macías, J., Løvholt, F., Selva, J., Volpe, M., et al. (2020). Probabilistic Tsunami Hazard Analysis: High Performance Computing for Massive Scale Inundation

Simulations. *Frontiers in Earth Science* 8. Available at: https://www.frontiersin.org/articles/10.3389/feart.2020.591549 [Accessed September 14, 2022].

Grezio, A., Babeyko, A., Baptista, M. A., Behrens, J., Costa, A., Davies, G., et al. (2017). Probabilistic Tsunami Hazard Analysis: Multiple Sources and Global Applications. *Reviews of Geophysics* 55, 1158–1198. doi: 10.1002/2017RG000579.

Lynett, P. J., Gately, K., Wilson, R., Montoya, L., Arcas, D., Aytore, B., et al. (2017). Inter-model analysis of tsunami-induced coastal currents. *Ocean Modelling* 114, 14–32. doi: 10.1016/j.ocemod.2017.04.003.

Lloyd, S. (1982). Least squares quantization in PCM. *IEEE Transactions on Information Theory* 28, 129–137. doi: 10.1109/TIT.1982.1056489.

Lorito, S., Selva, J., Basili, R., Romano, F., Tiberti, M. M., and Piatanesi, A. (2015). Probabilistic hazard for seismically induced tsunamis: accuracy and feasibility of inundation maps. *Geophysical Journal International* 200, 574–588. doi: 10.1093/gji/ggu408.

Løvholt, F., Bondevik, S., Laberg, J. S., Kim, J., and Boylan, N. (2017). Some giant submarine landslides do not produce large tsunamis. *Geophysical Research Letters* 44, 8463–8472. doi: 10.1002/2017GL074062.

Macías, J., Castro, M. J., and Escalante, C. (2020a). Performance assessment of the Tsunami-HySEA model for NTHMP tsunami currents benchmarking. Laboratory data. *Coastal Engineering* 158, 103667. doi: 10.1016/j.coastaleng.2020.103667.

Macías, J., Castro, M. J., Ortega, S., Escalante, C., and González-Vida, J. M. (2017). Performance Benchmarking of Tsunami-HySEA Model for NTHMP's Inundation Mapping Activities. *Pure Appl. Geophys.* 174, 3147–3183. doi: 10.1007/s00024-017-1583-1.

Macías, J., Castro, M. J., Ortega, S., and González-Vida, J. M. (2020b). Performance assessment of Tsunami-HySEA model for NTHMP tsunami currents benchmarking. Field cases. *Ocean Modelling* 152, 101645. doi: 10.1016/j.ocemod.2020.101645.

Pedregosa, F., Varoquaux, G., Gramfort, A., Michel, V., Thirion, B., Grisel, O., et al. (2011). Scikit-learn: Machine Learning in Python. *MACHINE LEARNING IN PYTHON*.

Perini, L., Calabrese, L., Luciani, P., Olivieri, M., Galassi, G., and Spada, G. (2017). Sea-level rise along the Emilia-Romagna coast (Northern Italy) in 2100: scenarios and impacts. *Natural Hazards and Earth System Sciences* 17, 2271–2287. doi: 10.5194/nhess-17-2271-2017.

Rafliana, I., Jalayer, F., Cerase, A., Cugliari, L., Baiguera, M., Salmanidou, D., et al. (2022). Tsunami risk communication and management: Contemporary gaps and challenges. *International Journal of Disaster Risk Reduction* 70, 102771. doi: 10.1016/j.ijdrr.2021.102771.

Selva, J., Tonini, R., Molinari, I., Tiberti, M. M., Romano, F., Grezio, A., et al. (2016). Quantification of source uncertainties in Seismic Probabilistic Tsunami Hazard Analysis (SPTHA). *Geophysical Journal International* 205, 1780–1803. doi: 10.1093/gji/ggw107.

Selva, J., Lorito, S., Volpe, M. *et al.* Probabilistic tsunami forecasting for early warning. *Nat. Commun*. 12, 5677 (2021). https://doi.org/10.1038/s41467-021-25815-w

Selva, J., Amato, A., Armigliato, A., Basili, R., Bernardi, F., Brizuela, B., ... & Zaniboni, F. (2021). Tsunami risk management for crustal earthquakes and non-seismic sources in Italy. *La Rivista del Nuovo Cimento*, *44*(2), 69-144.

Sepúlveda, I., Liu, P. L.-F., and Grigoriu, M. (2019). Probabilistic Tsunami Hazard Assessment in South China Sea With Consideration of Uncertain Earthquake Characteristics. *Journal of Geophysical Research: Solid Earth* 124, 658–688. doi: 10.1029/2018JB016620.

Tonini, R., Di Manna, P., Lorito, S., Selva, J., Volpe, M., Romano, F., et al. (2021). Testing Tsunami Inundation Maps for Evacuation Planning in Italy. *Frontiers in Earth Science* 9. Available at: https://www.frontiersin.org/articles/10.3389/feart.2021.628061 [Accessed June 28, 2023].

Volpe, M., Lorito, S., Selva, J., Tonini, R., Romano, F., and Brizuela, B. (2019). From regional to local SPTHA: efficient computation of probabilistic tsunami inundation maps addressing near-field sources. *Natural Hazards and Earth System Sciences* 19, 455–469. doi: 10.5194/nhess-19-455-2019.

Williamson, A. L., Rim, D., Adams, L. M., LeVeque, R. J., Melgar, D., and González, F. I. (2020). A Source Clustering Approach for Efficient Inundation Modeling and Regional Scale Probabilistic Tsunami Hazard Assessment. *Frontiers in Earth Science* 8. Available at: https://www.frontiersin.org/articles/10.3389/feart.2020.591663 [Accessed June 28, 2023].

Corresponding author: enrico.baglione@ingv.it

Comparison between alarm-based and probability-based earthquake forecasting methods

E. Biondini[1] and P. Gasperini[1,2]

[1] Dipartimento di Fisica e Astronomia, Università di Bologna, Italy
[2]Istituto Nazionale di Geofisica e Vulcanologia, Sezione di Bologna, Italy

In a recent work, we applied the Every Earthquake a Precursor According to Scale (EEPAS) probabilistic model to the pseudo-prospective forecasting of shallow earthquakes with magnitude $M \geq 5.0$ in the Italian region (Biondini et al., 2023). We compared the forecasting performance of EEPAS with that of the epidemic type aftershock sequences (ETAS) forecasting model, using the most recent consistency tests (Bayona et al., 2022) developed within the Collaboratory for the Study of Earthquake Predictability (CSEP). The application of such models for the forecasting of Italian target earthquakes seems to show peculiar characteristics for each of them. In particular, the ETAS model showed higher performance for short-term forecasting, in contrast, the EEPAS model showed higher forecasting performance for the medium/long-term. In this work, we compare the performance of EEPAS and ETAS models with that obtained by a deterministic model based on the occurrence of strong foreshocks (FORE model) using the alarm-based approach as described in Gasperini et al., (2021). We apply the two rate-based models (ETAS and EEPAS) estimating the best probability threshold above which we issue an alarm. The model parameters and probability thresholds for issuing the alarms are calibrated on a learning data set from 1990 to 2011 during which 27 target earthquakes have occurred within the analysis region. The pseudo-prospective forecasting performance is assessed on a validation data set from 2012 to 2021, which also comprises 27 target earthquakes. Tests to assess the forecasting capability demonstrate that, even if all models outperform a purely random method, which trivially forecast earthquakes proportionally to the space-time occupied by alarms, the EEPAS model exhibits lower forecasting performance than ETAS and FORE models. In addition, the relative performance comparison of the three models demonstrates that the forecasting capability of the FORE model appears slightly better than ETAS, but the difference is not statistically significant as it remains within the uncertainty level. However, truly prospective tests are necessary to validate such results, ideally using new testing procedures allowing the analysis of alarm-based models, not yet available within the CSEP.

References

Bayona, J. A., W. H. Savran, D. A. Rhoades, and M. J. Werner, 2022, Prospective evaluation of multiplicative hybrid earthquake forecasting models in California, Geophysical Journal International, 229, no. 3, 1736–1753, doi: 10.1093/gji/ggac018.

Biondini, E., D. A. Rhoades, and P. Gasperini, 2023, Application of the EEPAS earthquake forecasting model to Italy, Geophysical Journal International, ggad123, doi: 10.1093/gji/ggad123.

Gasperini, P., E. Biondini, B. Lolli, A. Petruccelli, and G. Vannucci, 2021, Retrospective short-term forecasting experiment in Italy based on the occurrence of strong (fore) shocks, Geophysical Journal International, 225, no. 2, 1192–1206, doi: 10.1093/gji/ggaa592.

Corresponding author: emanuele.biondini2@gmail.com

Imprints of the Earth's gravity on recent seismic events in Ceneselli, Italy

M. Campion[1], C. Fidani[2,3]

[1] *Gruppo Astrofili Polesani, Rovigo, Italy*
[2] *Istituto Nazionale di Geofisica e Vulcanologia, Roma, Italy*
[3] *Cenrtral Italy Electromagnetic Network, Fermo, Italy*

A laborious mechanical manufacture for the realization of a gravimeter was initiated at the beginning of 2000. The instrument manufacturer, Mario Giorgio Campion, put the gravimeter into operation at his home in via Arturo Toscanini 27 in Rovigo, Italy. The gravimeter is made up of a highly precise pendulum with damped oscillations: an integral accelerometer, which is able to detect oscillation times with precision and continuity (Campion, 2022). It was realized using materials and construction techniques to obtain the maximum rigour in the measurement of the variable (see Figure 1):

- it works under vacuum;
- with thermostatation;
- use rods in quartz and/or invar steel;
- synchronism with the focused laser;
- signals go throungh an optical fiber;
- times measured with a Rubidium clock;
- a computer controls and records data.

With these solutions, the variations of the period with respect to temperature were verified to be of the order of 1.65 μsec/°C. Through approximately 500 daily measurements, the instrument is able to measure local relative gravity continuously, over very narrow time intervals of approximately three minutes. Starting from 2000, the relative gravity recording went on for at least a decade; alternating intervals of stops of the gravimeter. The maintenance periods were useful in order to make necessary improvements to the system, therein reducing errors in the measurements both of random and systematic nature. This period was also useful to better understand the character of the captured data regarding the fundamental quantity of the gravity dependent on the mass of the Earth. Moreover, gravity is influenced by the nature of the subsoil, as well as by the geographical position of the location, and the altitude of the ground.

Fig. 1 – One of the damped pendulums self-built by Mario Campion in his laboratory. Note the vacuum pump connected to the base of the pendulum where the thermostat system is also located. The glass vacuum cylinder surrounds the pendulum made of invar steel. At the lower end of the rod there is a mass and the precision optical reading system of the instrument, this is connected via an optical fiber to the external rubidium clock.

As an element of credibility to validate the ability to record the gravity variations, the gravity trends, reconstructed starting from the measurements of this gravimeter, were compared to the tidal forces. The findings from a comparison carried out between the measurements of the damped pendulum and the tides is reported on the two plots of Fig. 1. Recordings concern the day 10 December 2019, 2 days before the New Moon, which were made simultaneously with two separate gravimeters, operating a few metres from each other with different oscillator periods. The traces in red on the graphs show the coincidence of the two maximums and the two minimums, both with the tide levels in Venice Lido, as well as with each other. Tide levels in Venice Lido were seen to have coincided exactly with the tide forces acting on the same location, most likely due to the complex resonance of the Adriatic Sea. Indeed, the plots do not show tide accelerations, but instead average oscillation times, this is because times are measured by damped oscillator through a focalized laser emitter detected by a Rubidium atomic clock. The period measure is also the motivation for measuring only a relative value of the gravity. In fact, the absolute value requiring the Kater's configuration would need repeated precise measurements of lengths (Lenzen and Multauf, 1964) which inevitably would lengthen measurement repetition times. Standard deviation of hourly averaged periods shown in Fig. 1 are a few units over ten millions. Its correspondent standard deviation on the gravity acceleration can be evaluated by

$$\Delta g/g=\Delta L/L+2\Delta T/T \quad (1)$$

where L (1 m) is the pendulum length and T (1.53 and 1.57 sec) the measured period. Being the pendulum under vacuum with thermostated (0.01 °C) quartz arm, $\Delta L/L < 10^{-8}$, Δg can be

evaluated by (1) in about 0.42 mGal for the gravimeter A on the top of Fig. 1, and in about 0.21 mGal for the

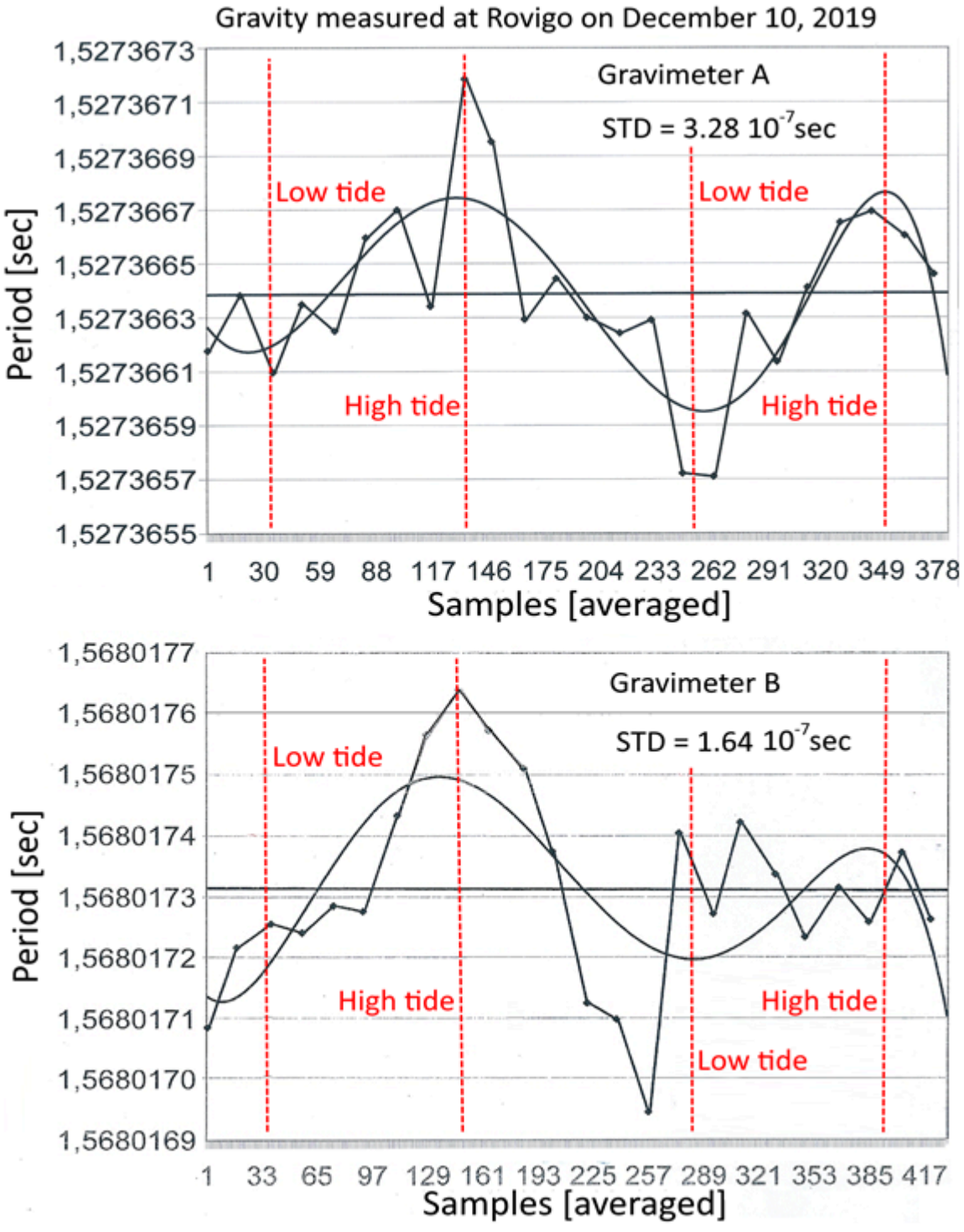

Fig. 2 – Two pendulum period recordings on December 10, 2019, where broken lines represent the union of the averaged points, continuos lines represent polynomial best fits, while red vertical dashed lines indicate tide phases at Venice Lido

gravimeter B on the bottom of Fig. 2. It should be highlighted that these are not the errors of the instruments as such standard deviations contain the tide contributions. The two graphs show on the abscissa the 378 and 417 measurements in the times of execution of the two gravimeters and on the ordinate the 24 values of the hourly averages joined by broken lines. Polynomial fits of the averaged periods are also reported to retrieve maximum and minimum periods corresponding to minimum and maximum gravity values, respectively. These graphs involve simultaneity and repetitiveness in the measurements of tidal forces validated by water levels in Venice on the same day and have surprised leading experts in the field of tidal study and tidal force recording.

Gravity data referred to a geographical point on Earth surface, which is usually a stable value, in turn is integrated with the addition of many very small perturbations. Generally of a transitory nature, small perturbations are observed to be induced by gravitational influences of the other celestial bodies of the solar system with greater mass (Campion, 2022), such as Jupiter and Saturn and/or from greater proximity such as Venus. These terrestrial gravity variations are difficult to determine with current gravimeters in a continuous way as they present variations in the sixth and seventh decimal of the period. Moreover, whenever detected in a sufficiently rigorous manner, gravity variations can provide valuable astronomical information. A further case concerns the ability of the damped pendulum gravimeter to highlight seismic events. It was used to record the gravity of the ground before, during, and after an earthquake highlighting some peculiar variations which were more intense during strong quakes (Campion, 2022).

Polesine had always been considered an area with low seismic risk, but the strong earthquake in Modena, Italy in 2012, which affected the upper part on the border with Emilia and Lombardy, suggested that this was not the case. The signal reported in Fig. 3 top coincided with the seismic shock of 17 July 2011 in Ceneselli, 33 km away from Rovigo, towards Lombardy, having a magnitude ML = 4.5 without causing any particular damage. The double recording of the event in Rovigo, with both the seismograph and the gravimeter, provided the possibility to observe the event in depth by integrating the information obtained with the two measurement systems. The two graphs were drawn vertically on the same Fig. 3 top, the seismogram upward and the gravity diagram downward, making the times of the two signals coincide, so as to carry out a comparison. The recording made by the seismograph produced the main wave detected by the gravimeter, while the second part of the same recording was attributable to the return to equilibrium of the ground. The first part of the gravimeter recording from 19:41:57 to 20:27:35, for a total of 45 minutes, shows three regular oscillations of the ground which were followed by a flat trend in gravity. The gravity flattening that preceded the seismic event could be interpreted as a sign of soil stretching and the critical phase before the shock. The shock itself, which seismic recording showed to last approximately 7 minutes, corresponds to a direct wave of the ground lasting 5 minutes and a reverse wave lasting 2 minutes, as measured by the gravimeter. Direct and reverse waves are due to the integration of seismic oscillations with the damped pendulum oscillations, these waves seem to indicate a first phase of gravity reduction followed by a rebound phase of gravity increases. A series of larger fluctuations followed the end of the event.

An earthquake of magnitude ML = 4.2 struck the area 1 km E in Ceneselli, on October 28, 2023, at 17:29:23 Italian time with geographical coordinates 45.015N, 11.388E at a depth of 8 km. The area affected by this earthquake was characterised by medium seismic danger and by strong earthquakes that had occurred in the past (INGV, 2015). The epicentre appears to fall in an area with few known earthquakes: the 2011 event discussed above, the sequence in the Po Valley in May-June 2012, and another event of magnitude ML = 4.2 occurred on October 25, 2023. The

measured period is reported in Fig. 3 bottom, it appeared to grow persistently for about half an hour before this minor event, which corresponded to a gravity decrease.

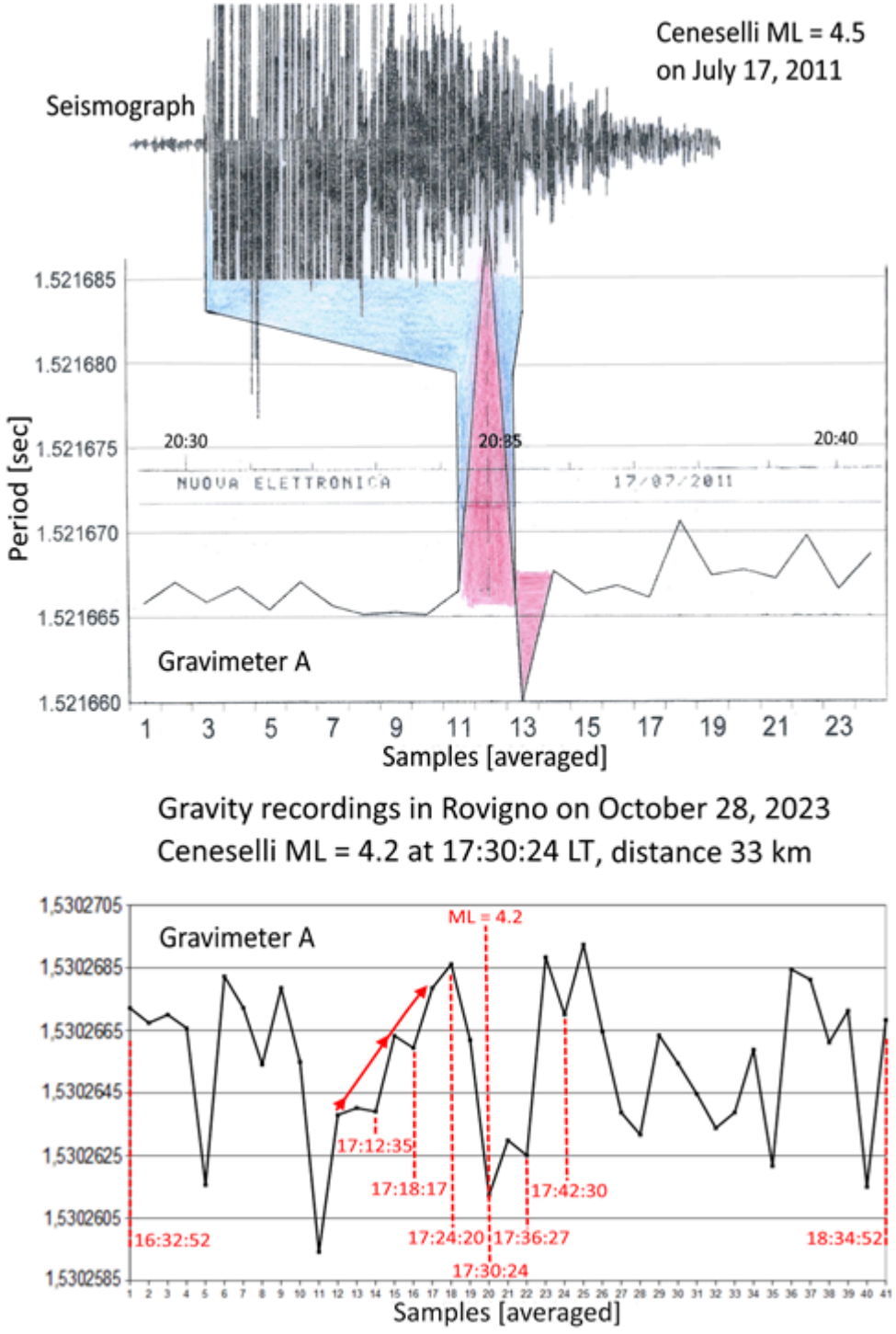

Fig. 3 – A gravity recording of the two hours between the seismic event occurred in Ceneselli on July 17, 2011. The seismogram recorded at the same position of the damped pendulum is reported on the top, where the blue area highlights the seismogram length while the red areas highlight direct and reverse gravimeter responses. Another gravity recording of the two hours between the seismic event occurred in Ceneselli on October 28, 2023, on the bottom. The gravity measurements are indicated by a broken line where the thick line indicates its average trend. Red areas evidence a trend of an increasing period that anticipated the shock, then the period suddenly decreased

References

Campion M.; 2022: Quanto ci può rivelare il tenue sussurro della gravità terrestre? Booksprint (13 Dec. 2022), p. 71.

INGV; 2015: CPTI15, Catalogo Parametrico dei Terremoti Italiani 2015, versione 4.0.

Lenzen V.F., Multauf R.P.; 1964: Development of gravity pendulums in the 19th century. United States National Museum Bulletin 240: Contributions from the Museum of History and Technology reprinted in Bulletin of the Smithsonian Institution. Paper 44. Washington: Smithsonian Institution Press., p. 307.

A data-driven parametrization of source-directivity effects: the study case of Central Italy

L. Colavitti [1,2], G. Lanzano [1], S. Sgobba [1], F. Pacor [1]

1 *National Institute of Geophysics and Volcanology, INGV*
Seismology applied to Engineering (Milan, Italy)
2 *University of Genoa, DISTAV*
Department of Earth, Environment and Life Sciences (Genoa, Italy)

INTRODUCTION

Assessing the spatial variability of seismic shaking in the epicenter zone is one of the major challenges to be addressed in seismic hazard estimates and ground motion scenarios generation. Among the various contributions causing the azimuthal variation of the shaking, source directivity plays a crucial role. As already proven by recent research, directivity effects, which are related to the characteristics of rupture propagation along the fault, can provoke ground motion amplifications in wider or narrower frequency ranges, even in small to moderate magnitude earthquakes (López-Comino et al., 2012; Pacor et al. 2016; Convertito et al. 2016). The scope of this work is to construct a fully data-driven directivity predictive model that can be used to estimate seismic ground motion amplification, using few independent parameters.

DATA AND METHOD

The dataset used in this research is the same used by Sgobba et al. (2021a) and Colavitti et al. (2022) and is formed by high-quality waveforms of Central Italy covering the period range from 2009 to 2018. In particular, we analyzed about 35,000 recordings from 460 stations (**Fig. 1a**) and 456 events (**Fig. 1b**), for which we computed the 5% acceleration elastic response spectra ordinates from 0.04 to 2 sec for shallow active crustal events (Spallarossa et al., 2023). The events spans from magnitude values between 3.2 and 6.5, and contain earthquakes of the sequence of L'Aquila in 2009 (Ameri et al., 2009; Calderoni et al., 2015) and Amatrice-Visso-Norcia in 2016-2017 (Chiaraluce et al., 2017; Michele et al., 2020).

The method to detect the effects of source directivity is the same implemented for the ordinates of the Fourier Amplitude Spectra (FAS) by Colavitti et al. (2022) and is based on the analysis of the residuals obtained from non-ergodic ground motion modelling. In particular, we identify the

systematic contributions of event, source, site and path effects thanks to a mixed effect calibration technique (Stafford, 2014). As already noted by Sgobba et al. (2023), the exceptional amount of information that has been produced in Central Italy, makes this area particularly suitable for a calibration of this kind of model.

The model calibrated in this study is a modified version of the one developed by Sgobba et al. (2021a) for the Central Italy and presents the following functional form:

$$log_{10}Y = a + F_M(M) + F_R(M,R) + \delta B_e + \delta S2S_s + \delta L2L_{source} + \delta P2P_p + \delta W_0 \quad [1]$$

where Y is the intensity measure, i.e. PGA or a spectral parameter (69 values logarithmically equispaced from 0.04 to 2 sec), a, $F_M(M)$, $F_R(M,R)$ are the fixed effects depending on magnitude M and distance metric R, while δB_e, $\delta S2S_{ref,s}$, $\delta P2P_p$ represents the zero-mean gaussian-distributed random effects.

Details on the fixed and random terms were provided in the paper of Sgobba et al. (2021); this study is based on the analysis of the azimuthal distribution of the leftover residual δW_0, which reflects the aleatory variability, net to the computation of the systematic effects. The azimuthal variation δW_0 is fitted starting from the general expression of the directivity factor C_d by Boatwright (2007):

$$C_d = \sqrt{\frac{k^2}{[1-(\frac{v_r}{c})cos(\theta-\theta_0)]^2} + \frac{(1-k)^2}{[1+(\frac{v_r}{c})cos(\theta-\theta_0)]^2}} \quad [2]$$

where $\frac{v_r}{c}$ is the Mach number from here on called α, θ_0 is the azimuth of the rupture direction and parameter k which spans from 0 to 1 indicates the relative portion of the rupture length along the rupture direction θ_0.

Taking into account that there is a trade-off between the fit parameters as α, k, θ and n, we have to assume fixed some of these values in order to vary others. After several tests, for this work we decided to fix k to 0.85 and α to 0.50 and then evaluating the directivity power by the parameter n. The constrained parameters are consistent with those reported in the literature (Ren et al., 2017; Convertito et al., 2017) and also ensure that we have a good fit in the majority of the events.

For the identification of directivity effects, we adopted the same criteria of Colavitti et al. (2022), which is based on these following points:

1. The coefficient of determination R^2 computed between the observed distribution of the aleatory residual δW_0 and the fit considering the C_d model is greater than 0.50 for at least 7 out of 69 periods investigated;

2. The standard deviation of the distribution of azimuths where n is maximized angle, θ_0, across all the vibration periods is smaller than 20°.

RESULTS

With the proposed methodology, we identified 175 out of 456 (38%) directive events that exhibits a clear azimuthal pattern and frequency dependence, representing the signature of source directivity. Comparison with the previous analysis in FAS shows that the directivity analysis carried out in SA extends to wider bands and that the directivity peak itself, defined by the value of n_{max}, is always higher than the corresponding peak in SA.

For directivity modelling, we focus on the spectral trend of the n parameter, which experimentally showed a curve that can be fitted with a Gaussian distribution, with the maximum value of n, n_{max} and the corresponding period called $T_{n_{max}}$. Since according to Colavitti et al. (2022) $T_{n_{max}}$ depends on the magnitude and the amplitude of n_{max} is proportional to the "strength" of the directivity, we need to normalize the parametrization curve for $T_{n_{max}}$ (period of the peak of the directivity) and n_{max} (the peak itself).

The normalized curves are shown in **Figure 1** and represent on average a Gaussian-like pattern with non-negligible variability. We decided to adopt a fit model based on a Gaussian distribution of order 1 which is defined by the following equation:

$$\frac{n}{n_{max}} = a_1 * exp^{\left(-\frac{\left(log_{10}\left(\frac{T}{T_{n_{max}}}\right)-b_1\right)}{c_1}\right)^2} \quad [3]$$

where $\frac{n}{n_{max}}$ represents the function to parametrize with respect to the x parameter (where $x = log_{10}\frac{T}{T_{n_{max}}}$), a_1 is the amplitude, b_1 the median value along x and c_1 is a coefficient that controls the width of the gaussian distribution bell. **Figure 1** shows the fit according to the first-order Gaussian constraining the model with $\frac{n}{n_{max}} = 1$ and $log_{10}\frac{T}{T_{n_{max}}} = 0$. In this way, c_1 is equal to 0.8229, which is the value for the median curve considering all the events.

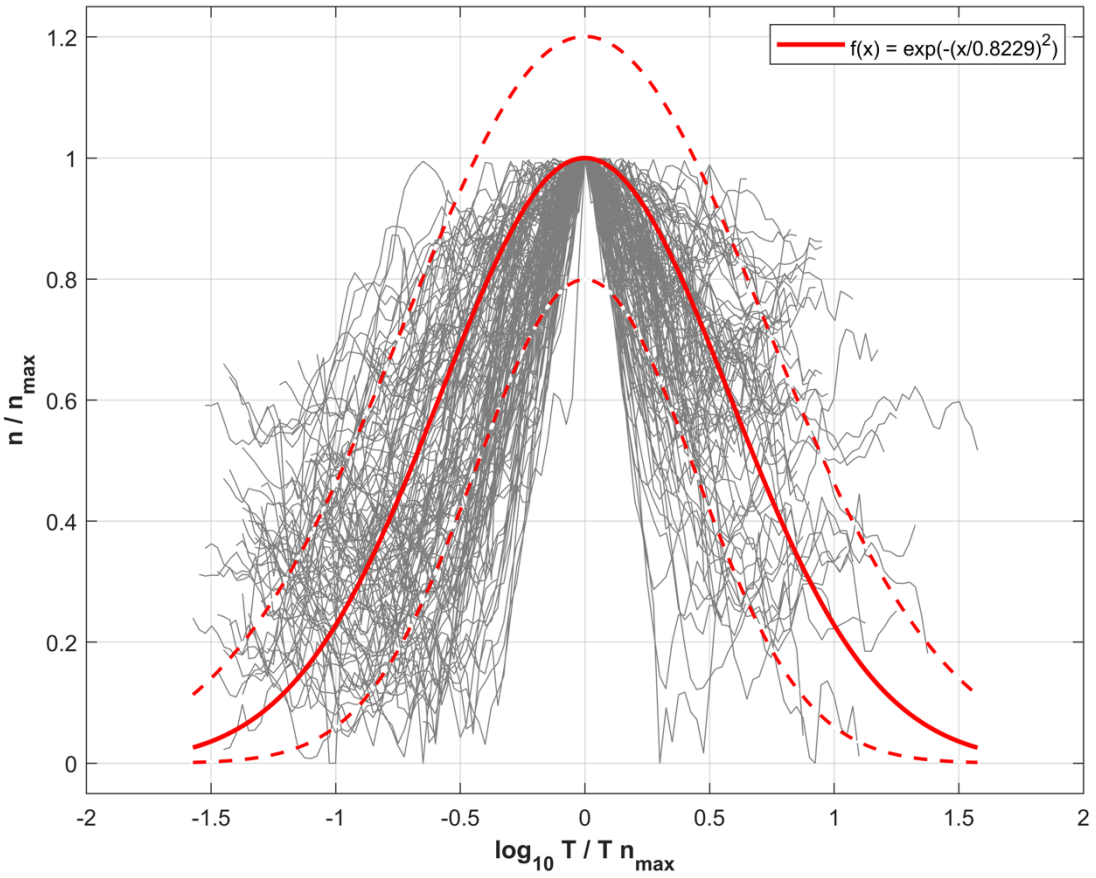

Figure 1. Relation between $\frac{n}{n_{max}}$ and $log_{10}\frac{T}{T_{n_{max}}}$ fitted with a Gaussian curve of order 1 and forcing the peak to the point 0,1. Grey lines are the events observed, red solid curve represents the best fit, while the standard deviation is shown by the red dashed curves. Some statistical parameters of the Gaussian: $c_1 = 0.8229$, fit $R^2 = 0.7822$, error $RMS = 0.0597$ and standard deviation $\sigma = 0.1980$.

CONCLUSIONS AND FUTURE PERSPECTIVES

Based on equation [3], we are able to provide a preliminary spectral parametrization of the amplitude of the source directivity, adopting a simple functional form with input values of $T_{n_{max}}$ and n_{max}. Based on several empirical models (see Sgobba et al., 2021b), $T_{n_{max}}$ is function of magnitude whereas the bandwidth can be modelled as directly proportional to the "strength" of the directivity.

At this stage, shaking scenarios in Central Italy can be generated including directivity contributions using non-ergodic ground motion models, once that the direction of rupture propagation and the level of source directivity is assumed *a priori*.

A future perspective of this work could be to extend the method into different tectonic contexts (e.g. 2019 Ridgecrest earthquake sequence, on a strike-slip fault domain) where we have a huge amount of recordings available and different styles of faults.

Acknowledgements

We are very grateful to Prof. Daniele Spallarossa (University of Genoa, Italy) for making available the dataset used in this work and to Prof. František Gallovič (University of Prague, Czech Republic) for the fruitful discussion about this work. This research is supported by the Italian Ministry of University and Research (MIUR) in the frame of the project SECURE: "Regional-Scale Earthquake Ground Motion PrediCtions ThroUgh Pyhsics-based and EmpiRical ApproachEs: A Case study Central Italy".

References

Ameri G., Massa M., Bindi D., D'Alema E., Gorini A., Luzi L., Marzorati S., Pacor F., Paolucci R., Puglia R., Smerzini C.; 2009.
The 6 April 2009 Mw 6.3 L'Aquila (central Italy) earthquake: Strong-motion observations. Seismol. Res. Lett., 80(6), 951-966. https://doi.org/10.1785/gssrl.80.6.951.

Boatwright J.; 2007. The persistence of directivity in small earthquakes. Bull. Seismol. Soc. Am., 97, 1850-1861. https://doi.org/10.1785/0120050228.

Calderoni G., Rovelli A., Ben-Zion Y. and Di Giovambattista R.; 2015. *Along-strike rupture directivity of earthquakes of the 2009 L'Aquila, Central Italy, seismic sequence.* Geophys. J. Int., 205, 399-415. https://doi.org/10.1093/gji/ggv275.

Chiaraluce L., Di Stefano R., Tinti E., Scognamiglio L., Michele M., Casarotti E., Cattaneo M., De Gori P., Chiarabba C., Monachesi G., Lombardi A., Valoroso L., Latorre D., Marzorati S.; 2017. *The 2016 central Italy seismic sequence: A first look at the mainshocks, aftershocks, and source models.* Seismol. Res. Lett., 88(3), 757-771. https://doi.org/10.1785/0220160221.

Colavitti L., Lanzano G., Sgobba S., Pacor F. and Gallovič F.; 2022. *Empirical evidence of frequency-dependent directivity effects from small-to-moderate normal fault earthquakes in Central Italy*. J. Geophys. Res: Solid Earth, 127, e2021JB023498. https://doi.org/10.1029/2021JB023498.

Convertito V., Pino N. A. and Di Luccio F.; 2010. *Investing source directivity of moderate earthquakes by multiple approach: The 2013 Matese (southern Italy) Mw=5 event.* Geophys. J. Int., 207, 1513–1528. https://doi.org/10.1093/gji/ggw360.

Convertito V., De Matteis R., Pino A.; 2017. *Evidence for static and dynamic triggering of seismicity following the 24 August 2016 Mw = 6.0, Amatrice (Central Italy) earthquake.* Pure and Appl. Geophys.,174, 3663-3672. https://doi.org/10.1007/s00024-017-1559-1.

López-Comino J. A., de Lis Mancilla F., Morales J. and Stich D.; 2012. Rupture directivity of the 2011, Mw 5.2 Lorca earthquake (Spain). Geophys. Res. Lett., 39, L03301. https://doi.org/10.1029/2011GL050498.

Michele M., Chiaraluce L., Di Stefano R. and Waldhauser F.; 2020. *Fine-Scale Structure of the 2016-2017 Central Italy Seismic Sequence from Data Recorded at the Italian National Network.* J. Geophys. Res.: Solid Earth, 125, e2019JB018440. https://doi.org/10.1029/2019JB018440.

Pacor F., Gallovič F., Puglia R., Luzi L. and D'Amico M.; 2016. *Diminishing high-frequency directivity due to a source effects: Empirical evidence from small earthquakes in the Abruzzo region, Italy*. Geophys. Res. Lett: Solid Earth, 43, 5000-5008. https://doi.org/10.1002/2016gl068546.

Ren Y., Wang H. and Wen R.; 2017. *Imprint of rupture directivity from ground motions of the 24 August 2016 Mw6.2 Central Italy earthquake.* Tectonics, 36, 3178-3191. https://doi.org/10.1002/2017tc004673.

Sgobba S., Lanzano G. and Pacor F.; 2021a. Empirical nonergodic shaking scenarios based on spatial correlation models: An application to central Italy. *Earthq. Eng. and Struct. Dynam*., 50(1), 60-80. https://doi.org/10.1002/eqe.3362.

Sgobba S., Felicetta C., Lanzano G., Ramadan F., D'Amico M., Pacor, F.; 2021b. *NESS2.0: An Updated Version of the Worldwide Dataset for Calibrating and Adjusting Ground-Motion Models in Near Source.* Bull. Seism. Soc. Am., 111(5), 2358-2378. https://doi.org/10.1785/0120210080.

Sgobba S., Lanzano G., Colavitti L., Morasca P., D'Amico M. C., Spallarossa D.; 2023. *Phyics-based parametrization of a FAS nonergodic ground motion model for Central Italy.* Bull. Earthq. Eng., 21, 4111-4137. https://doi.org/10.1007/s10518-023-01691-1.

Spallarossa D., Colavitti L., Lanzano G., Sgobba S., Pacor F., Felicetta C.; 2022. *CI-SA_Flatfile: Parametric table of the 5% Acceleration response Spectra ordinates and associated metadata for the shallow active crustal events in Central Italy (2009-2018)* [Data set]. Istituto Nazionale di Geofisica e Vulcanologia (INGV). https://doi.org/10.13127/CI_dataset/CI-SA_flatfile.

Stafford P. J.; 2014. *Crossed and nested mixed-effects approaches for enhanced model development and removal of the ergodic assumption in empirical ground-motion models.* Bull. Seism. Soc. Am., 104(2), 702-719. https://doi.org/10.1785/0120130145.

Corresponding author: leonardo.colavitti@edu.unige.it

Radon observations during the November 14 Montelparo, M = 4, and December 6 Allerona, M=3.6, earthquakes in 2023

G. De Antoni[1] C. Fidani[1,2,3,4] M. Siciliani[4] T. Milan[1]

[1] *Osservatorio Geofisico di Novara, Novara, Italy*
[2] *Istituto Nazionale di Geofisica e Vulcanologia, Roma, Italy*
[3] *Central Italy Electromagnetic Network, Fermo, Italy*
[4] *Osservatorio Sismico Andrea Bina, Perugia, Italy*

The Central Italy Electromagnetic Network (Fidani, 2011) was recently updated with a novel Radon detector (Fidani et al., 2022) developed by a project of the Novara Geophysical Observatory, at http://www.osservatorionovara.it/. A Radon detector prototype developed by the Novara Observatory team (De Antoni et al., 2011) was installed at the Fermo Station in January 2020. The installation followed the indications of the Novara Observatory team, which suggested to bury the pipe vertically with the bottom end open, and with the tube cap protruding a few cm from the ground. The scheme of the placement of the tube with a photo of the open cap is shown in Figure 1, note the bag that protects the sensor from condensation and the thermal insulating coating to reduce convective motions inside the pipe.

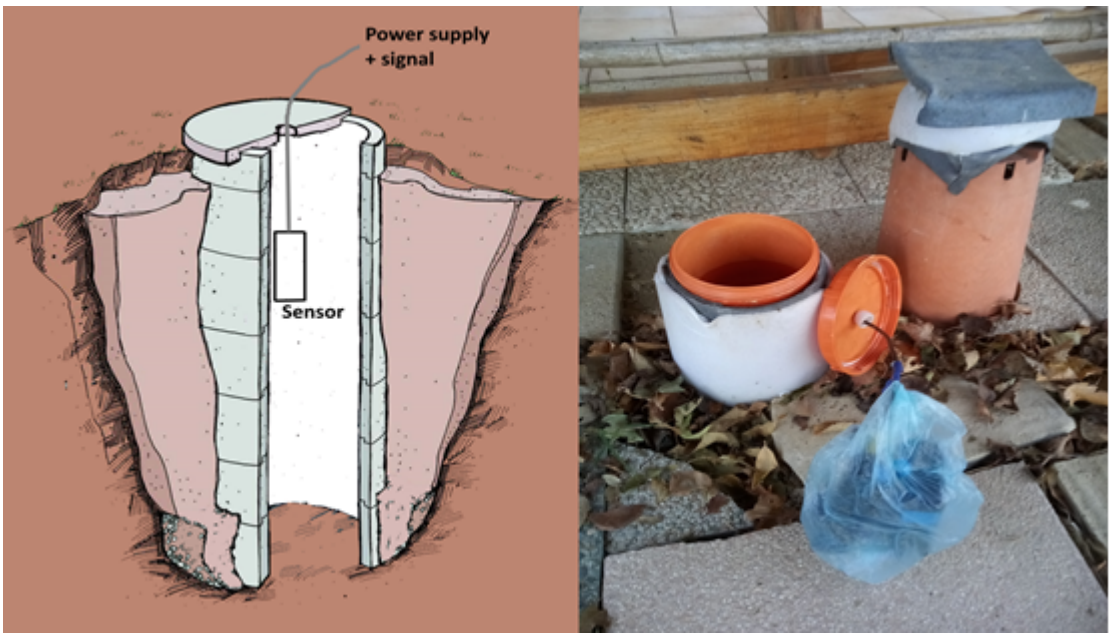

Fig. 1 – Scheme of the buried pipe with the sensor on the left, a photo of the top pipe open with the sensor placed outside on the right.

A year and half later, following the team indications, another three detectors were realized and installed; two in Gubbio and one at the Perugia Seismic Observatory Andrea Bina https://www.binapg.it/. The detectors are embedded in a network of observatories and have so far collected continuous recordings, separated by some interruptions due to the need for instrument maintenance, together with electric and magnetic detectors, gamma and air ions detectors, as well as meteorological stations https://cfidani.wixsite.com/cien. The objective of these instruments is to develop a physical model that links earthquake events to mutually interacting geophysical observables, in order to better understand the earthquake process manifested in the lowest surface atmosphere. Thus, for example, Radon escaping from the ground has been widely hypothesized to be driven by fluid migration towards the Earth's surface, and Radon plus fluids entering the atmosphere able to generate electromagnetic signals therein modifying meteorological conditions. Moreover, fluid migrations have been reported to be the primary trigger of Appennine earthquakes (Chiodini et al., 2004). Finally, the multi-parameter monitoring of the Central Italy Electromagnetic Network is mainly dedicated to the physical processes occurring on the ground-atmosphere interface.

Two moderately intense seismic events struck Central Italy between November-December 2023. An earthquake of magnitude ML = 4.0 occurred at about 3 km S Montelparo (Fermo), on November 14, 2023, 17:17:50 Italian time with geographical coordinates 42.996N and 13.537E at a depth of 21.6 km. The shock was generated by a compressional fault that is a typical mechanism of this area, due to the Apennine axis relaxation which towards the Adriatic Sea implicates a shortening belt. The area had been characterised by strong seismic events, as confirmed by the strong earthquakes of November 26, 1972, having an estimated magnitude Mw = 5.5, and of October 3, 1943, with an estimated magnitude Mw = 5.7 (INGV, 2015). The hourly decay counts of the 5 days preceding the November 14, 2023 shock are shown with a blue line in Fig. 2 bottom. Whereas, the red line in Fig. 2 bottom represents the 12-hour moving average of 12 previous counts reported in real time. Specifically, two decay increases are better visible by 12-hour moving averages, and these increases anticipated the seismic event indicated by a vertical red arrow in Fig. 2 bottom. The end of the smallest recorded average increase preceded the earthquake by two days, while the end of the largest recorded average increase preceded the earthquake by one day. The increases peak intensities were 30% for the smallest and of 120% for the largest. The meteorological instruments at the Fermo Station did not report any rain events or sudden pressure reductions during the peaks. However, a weak rain event registered prior to the quake was recorded between November 10th and 11th, 2023, with a cumulation of 7 mm.

These peaks were repeatedly detected before moderate seismic events at the Fermo Station. Furthermore, similar peaks were also detected before moderate seismic events in Central Italy by the stations located in Nepi (VT), Orvieto (TR), Campli (TE), and Gubbio (PG) http://www.osservatorionovara.it/. Other peaks and periodic variations having not been followed by moderate seismic events have been studied in relation to meteorological variables providing some interpretative agreement. Additional examples of increases, similar to those recorded a few days after the Montelparo event, occurred without any significant recorded seismic and meteorological events. On November 16, 2023, a sudden increase in the count decay was recorded to be 20 times the average, only to return to the initial value before the end of the same day, see Fig. 2 top. No rain or pressure variation events were recorded by the meteorological instruments before November 16. While a sudden and unexpected temperature

peak was recorded during the first hours of 17 November, 2023. The temperature peak reached 5 °C over a time interval during the early morning hours when the temperature is usually at its lowest. The time interval duration of around 4 hours from the 00:00 to 04:00 on November 17 is represented by a red line in Fig. 2 top, while the green line indicates the dew point. Data from the Montelparo meteorological instruments, and other stations positioned within 50 km, all reported significant increases in the temperatures during the same hours or over a longer time interval. Moreover, the temperatures recorded by meteorological stations more than 100 km from the Fermo Station did not detect any increases over the same hours. No increases in temperature were observed from Fig. 2 top after the December 13, 2023, peak.

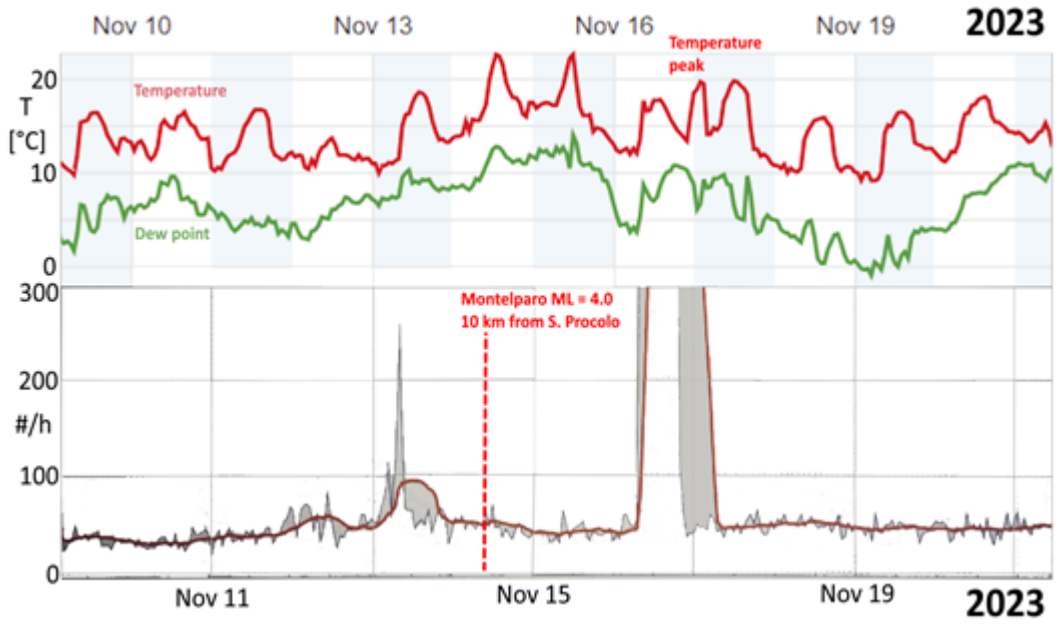

Fig. 2 – The Radon decay counts recorded at the San Procolo, Fermo Station, during the 5 days around the seismic event on the bottom, the temperature and the dew point trends along the same time interval on the top. The second recorded count decay peak is only partially shown here

An earthquake of a magnitude ML = 3.6 occurred 4 km SE Allerona (TR), on December 6, 2023, at 21:06:13 Italian time having geographical coordinates of 42.7960N and 12.0130E at a depth of 10.6 km (INGV, 2015). Its focal mechanism having been a strike sleep was unlike the Montelparo event. Strong earthquakes have occurred in the past in the same area although with a lower frequency than in the Marche Region. The active Radon detector nearest to the epicentre was the Perugia Seismic Observatory Andrea Bina https://www.binapg.it/, during the same period of the December 6 event, less than 50 km from the epicentre. The detector is located inside the San Pietro Abbey in Perugia and has been operative since the beginning of 2022. To date, this detector has counted an average low number of daily Radon decays, reaching a relative maximum on December 2, 2023. A relative minimum occurred about two day after the maximum on December 4, 2023, about two days before the shock, reported in Fig. 3. Pressure reported on the top of Fig. 3 evidenced a maximum of 1,019 mbar during the descending phase of the Radon count. Whereas, a 21 mm of cumulate rainfall was measured on December 5, 2023, and reported on the bottom of Fig. 3. No apparent influence of meteorological conditions on the Radon measurements were detected in Perugia over the same days. The data collected from both these recent events and all events in recent years proves to be valuable for testing the

monitoring network https://cfidani.wixsite.com/cien. This enables a statistical investigation into their correlation with seismic events.

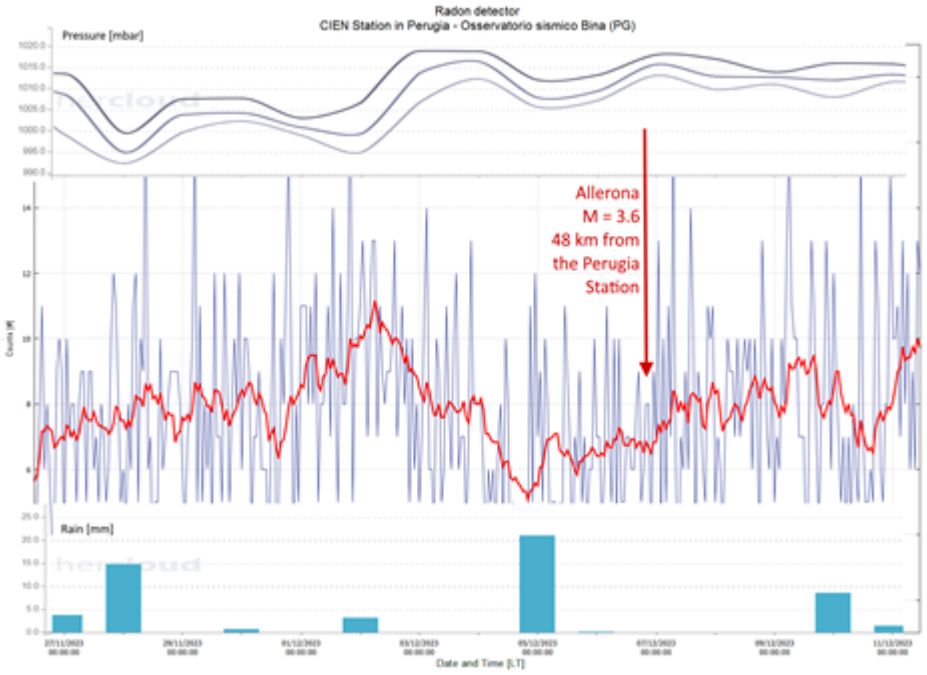

Fig. 3 – The Radon decay counts at the Andrea Bina Observatory, Perugia Station, measured during the days preceding and following the Allerona event, indicated by a vertical red arrow, and the superimposed meteorological trends of pressure on the top and rain on the bottom along the same time interval

References

Chiodini G., Cardellini C., Amato A., Boschi E., Caliro S., Frondini F., Ventura G.; 2004: Carbon dioxide Earth degassing and seismogenesis in central and southern Italy. Seismological Research Letters, 31, L07615.

De Antoni G., Milan T., Santini C., Baroffio E., Barile G.; Analisi della variazione del gas Randon lungo la Faglia della Cremosina e Sintesi sulla ricerca e sperimentazione di un nuovo sensore Radon. Osservatorio Geofisico di Novara, Progetto Gas Radon, pp. 40. http://www.osservatorionovara.it/1%20e%202%20Pubblicazione%20Radon.pdf

Fidani C.; 2011: The Central Italy electromagnetic network and the 2009 L'Aquila earthquake: observed electric activity. Geosciences, 1 (1), 3-25.

Fidani C., De Antoni G., Milan T., Siciliani M.; 2022: An update of the Central Italy Electromagnetic Network with Radon detectors, 40th GNGTS, Trieste, p. 47-51.

INGV; 2015: CPTI15, Catalogo Parametrico dei Terremoti Italiani 2015, versione 4.0.

Statistically interpreting multiple observations derived from one or more geophysical monitoring networks

C. Fidani[1,2]

[1] *Istituto Nazionale di Geofisica e Vulcanologia, Roma, Italy*
[2] *Cenrtral Italy Electromagnetic Network, Fermo, Italy*

Recent studies have unveiled significant statistical correlations between specific geophysical parameters and seismic activity. Statistical correlations for ULF geomagnetic fluctuations at ground stations have been calculated exclusively when considering moderate magnitude earthquakes (Schekotov et al., 2006). In alternative investigations, a lead time of 6–7 days for Pc1 was observed (Bortnik et al., 2008), VLF noise exhibited a lead time of 2 days (Oike and Yamada, 1994), lightning activities were noted to precede earthquakes by 17–19 days (Liu et al., 2015), and geoelectric fields demonstrated lead times ranging from days to weeks (An et al., 2020). A statistical correlation between earthquakes and VLF/LF signals, spanning approximately 10 years, was established using the Japanese VLF/LF network. The findings, as reported by Hayakawa et al. (2010), disclosed discernible perturbations in the signals occurring 3–6 days before the seismic wave paths. Low-orbit satellites provide the capability to observe extensive ground areas within a few hours, facilitating the monitoring of regions affected by seismic events. From this perspective, using the Intercosmos-24 satellite, Molchanov (1993) observed a 50% increase in the probability of charged particle burst observations occurring 6 to 24 hours before seismic events. Additionally, onboard the AUREOL-3 satellite, Parrot (1994) noted an augmentation in the average wave intensity correlated with seismic activity. The micro-satellite DEMETER enabled a statistical study of VLF electromagnetic wave intensity in the vicinity of earthquake epicenters (Nemec et al., 2008), evidencing a significant decrease in the measured wave intensity, 0–4 h before strong earthquakes. Analysing Total Electron Content (TEC) data from the global ionosphere map, researchers found that the highest occurrence rates of anomalies were associated with earthquakes of larger magnitudes and lower depths, 1–5 days before the seismic events (Zhu et al., 2018). This trend was corroborated by studies conducted in Japan (Kon et al., 2011) and China (Ke et al., 2016). Reports worldwide have documented concentrations of electron density and magnetic anomalies occurring more than two months to a few days before earthquake events (De Santis et al., 2019). Space-based observations have detected thermal infrared anomalies, and a comprehensive review by Tramutoli et al. (2015) has documented the major contributions and results achieved in over 30 years of correlating these anomalies with strong earthquakes. Finally, sudden variations in high-energy charged particles

have been linked to strong earthquakes, particularly during periods of low solar activity, as documented by Fidani (2015).

Currently, Earth is witnessing the development of numerous geophysical earth observation networks, each designed for specific purposes. These evolving networks aim to monitor various facets of our planet's geophysical activity. As highlighted above, recent findings suggest that many of these networks hold potential applications in earthquake studies. Satellite monitoring networks are implemented through various programs, including NOAA and MetOps, which focus on meteorological forecasting. Additionally, the Swarm constellation was operational for monitoring the geomagnetic field. Finally, Cses02 was scheduled to be launched after Cses01 was placed in orbit in 2018, creating a dedicated project for earthquake monitoring. A ground-based network is for example INTERMAGNET, see Fig. 1, a collaboration of digital magnetic observatories accessible at https://intermagnet.org/. INTERMAGNET adopts modern standard specifications for measuring and recording equipment, facilitating seamless data exchanges and the near real-time production of geomagnetic recordings. Furthermore, a long-term plan for the integration of existing national and trans-national research infrastructures for solid Earth science in Europe, EPOS at https://www.epos-eu.org/, sustains such a program through the utilisation of multidisciplinary solid Earth science data, data products, and services, along with physical access to facilities. It is in the process of developing a federated and sustainable research platform aimed at delivering coordinated access to harmonised and quality-controlled data spanning diverse Earth science disciplines. This platform will also offer tools for analysis and modelling. EPOS actively promotes global interoperability in Earth sciences and extends its services to a broad community of users. Such prospectives and discoveries have ignited a growing interest in investigating the feasibility of a comprehensive analysis that incorporates multiple parameters, both ground-based and space-based, to evaluate the occurrence of a seismic event.

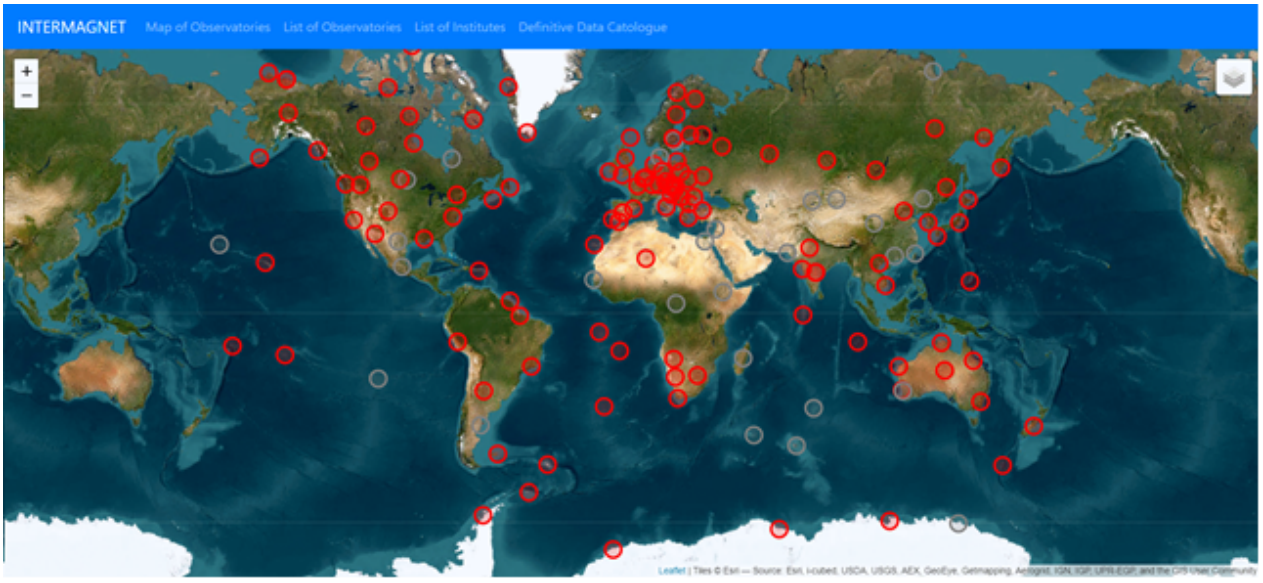

Fig. 1 – Map distribution of geomagnetic observatories belonging to INTERMAGNET programme, red circles represent active international magnetic observatories while gray circles represent closed observatories

Defining the conditional probability of a noteworthy event, like an earthquake, involves analysing the variations in a geophysical observable that typically precedes it. In this context, time series representation involves binary events, with '1' indicating instances where the observable exceeds a certain magnitude threshold. For instance, these events could be seismic activities surpassing a specific magnitude or any observable exceeding its defined threshold. Subsequently, the likelihood of an earthquake is assessed by examining the correlation between these binary events. Or also, a probability increase for an earthquake can be defined by the probability gain

$$G_A = P(EQ|EA)/P(EQ), \quad (1)$$

where P(EQ) represents the frequency of the earthquake event of a magnitude greater than a fixed value, and EA represents the observable A event, being the conditional probability

$$P(EQ|EA) = P(EQ) + corr(EQ,EA)\ \{P(EQ)[1-P(EQ)][1-P(EA)]/P(EA)\}^{½}, \quad (2)$$

defined by the Pearson Coefficient R = corr(EQ,EA) and the frequency of the event A, P(EA). Such a relation (2) for the probability gain due to the observable A is valid only for binary event series. Let's explore the scenario where we observe two quantities, drawing from existing networks like the electromagnetic network in central Italy and the network comprised of NOAA satellites. The first network records magnetic field pulses, while the second detects electron precipitation. The magnetic pulses have the potential to alter the trajectory of electrons reaching the ionosphere, indicating compatibility and dependence between the two observables. These quantities can be observed concurrently (represented by the symbol ⋂) or individually, without distinction (represented by the symbol U). The correspondent probability gains (Fidani, 2021)

$$G_{EB\cap MP} = P(EB\cap MP|EQ)/P(EB\cap MP), \quad (3)$$

where EB is the electron burst event and MP is the magnetic pulse event, which reduces to $G_{EB}G_{MP}$ if the events were compatible but completely independent, and

$$G_{EB\cup MP} = \frac{G_{EB}P(EB) + G_{MP}P(MP) - G_{EB\cap MP}P(EB)P(MP)}{P(EB) + P(MP) - P(EB\cap MP)}, \quad (4)$$

which reduces to $[G_{EB}P(EB) + G_{MP}P(MP) - G_{EB}G_{MP}P(EB)P(MP)]/[P(EB) + P(MP) - P(EB)P(MP)]$ if the events were compatible but completely independent. In the case of compatible and dependent events it will be necessary to evaluate correlations of the type corr(EQ,EB⋂MP), i.e. concerning the concurrence of EB and MP events.

Ultimately, these probability gains define the increase in conditional probabilities of the occurrence of an earthquake of a certain minimum magnitude compared to the observation of the two observables together or only one of the two, regardless of which. In a model verification scenario, the region where the alarm is activated is specified for each observable, as illustrated in Fig. 2, for instance. If this region is not identical for both observables, then the probability gains of the observables need to be recalculated within the shared area. In the presence of

different networks, we could use the two gains, G∩ and GU, depending on whether we consider the observables distinct or indistinguishable in the intersection areas. The same parameter measured at different stations is combined as two different observations. Finally, G(∩) increases for highly intercorrelated parameters and G(U) increases for slightly intercorrelated parameters, consequently forecasting probabilities are given.

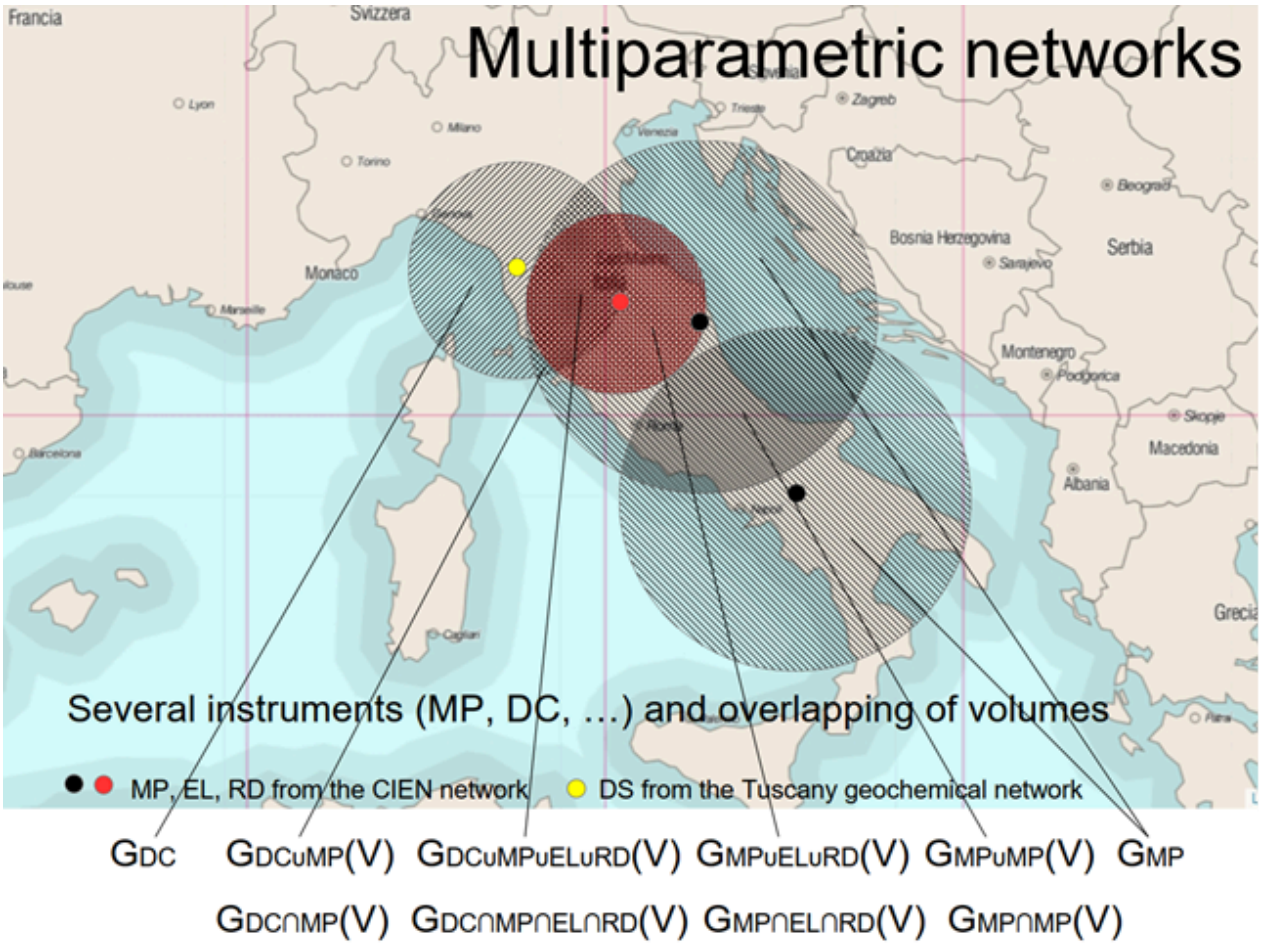

Fig. 2 – A potential scenario for testing a forecasting model in Italy involves leveraging the existing geophysical observational networks in the country

In summary, the verification process for this model is applicable to any observable, whether from ground-based or space-based sources. It necessitates the availability of geophysical observation datasets covering sufficiently long common time intervals. After establishing the elementary time interval, the initial step involves identifying anomalous events in the observable or, alternatively, events of interest, and assigning "1"s in the respective series. Subsequently, the series are correlated pairwise to identify any peaks. If correlation peaks are observed, the probability gains attributed to individual observables can be determined. From these gains, an attempt can be made to evaluate the probability gains resulting from data fusion. The process can be resumed in Fig. 3. The author thank the Limadou Scienza + (ASI) Project for the financial support.

Network	Observable	Studies of fluctuations	Binary series	Correlations	Conditional probabilities	Gains combined	Improved forecasting model
1) Seismic	... magnitude ...	Mo		1)-2) 1)-3)	P(1|2) P(1|3)	G2∩3 G2U3	P(1|2∩3)
2) A	1	threshold 1		2)-3)	Probability gains	using P(2|3)	P(1|2U3)
3) B	5 ...	threshold 2			G2 G3		

Fig. 3 – Steps of the process to improve forecasting

References

An Z., Zhan Y., Fan Y., Chen Q., Chen Q., Liu J.; 2019: Investigation of the Characteristics of Geoelectric Filed Earthquake Precursors: a Case Study of the Pingliang Observation Station, China. Ann. Geophys. 62 (5), 545.

Bortnik J., Cutler J. W., Dunson C., Bleier T. E.; 2008: The Possible Statistical Relation of Pc1 Pulsations to Earthquake Occurrence at Low Latitudes. Ann. Geophys. 26, 2825–2836.

De Santis A., Marchetti D., Pavón-Carrasco F. J., Cianchini G., Perrone L., Abbattista C., et al.; 2019: Precursory Worldwide Signatures of Earthquake Occurrences on Swarm Satellite Data. Sci. Rep. 9, 20287.

Fidani, C.; 2015: Particle Precipitation Prior to Large Earthquakes of Both the Sumatra and Philippine Regions: A Statistical Analysis. J. Asian Earth Sci. 114, 384–392.

Fidani C.; 2021: West Pacific Earthquake Forecasting Using NOAA Electron Bursts With Independent L-Shells and Ground-Based Magnetic Correlations. Front. Earth Sci. 9:673105.

Hayakawa M., Kasahara Y., Nakamura T., Muto F., Horie T., Maekawa S., et al.; 2010: A Statistical Study on the Correlation between Lower Ionospheric Perturbations as Seen by Subionospheric VLF/LF Propagation and Earthquakes. J. Geophys. Res. 115, A09305.

Ke F., Wang Y., Wang X., Qian H., Shi C.; 2016: Statistical Analysis of Seismo-Ionospheric Anomalies Related to Ms > 5.0 Earthquakes in China by GPS TEC. J. Seismol 20, 137–149.

Kon S., Nishihashi M., Hattori K.; 2011: Ionospheric Anomalies Possibly Associated with M≥6.0 Earthquakes in the Japan Area during 1998-2010: Case Studies and Statistical Study. J. Asian Earth Sci. 41, 410–420.

Liu J. Y., Chen Y. I., Huang C. H., Ho Y. Y., Chen C. H.; 2015: A Statistical Study of Lightning Activities and M ≥ 5.0 Earthquakes in Taiwan during 1993-2004.

Molchanov, O. A.; 1993: Wave and Plasma Phenomena inside the Ionosphere and Magnetosphere Associated with Earthquakes, in Review of Radio Science 1990–1992. Editor W Ross Stone (Oxford: Oxford University Press), 591–600.

Oike K., and Yamada T.; 1994: Relationship between Shallow Earthquakes and Electromagnetic Noises in the LF and VLF Ranges, in Electromagnetic Phenomena Related to Earthquake Prediction (Tokyo: Terra Scientific Publishing Company), 115–130.

Němec F., Santolík O., Parrot M., Berthelier J. J.; 2008: Spacecraft Observations of Electromagnetic Perturbations Connected with Seismic Activity. Geophys. Res. Lett. 35, L05109.

Parrot, M.; 1994: Statistical Study of ELF/VLF Emissions Recorded by a Low-Altitude Satellite during Seismic Events. J. Geophys. Res. 99 (A12), 339–347.

Schekotov A., Molchanov O. Hattori K., Fedorov E., Gladyshev V. A., Belyaev G. G., et al.; 2006: Seismo-ionospheric Depression of the ULF Geomagnetic Fluctuations at Kamchatka and Japan. Phys. Chem. Earth, Parts A/B/C 31, 313–318.

Tramutoli V., Corrado R., Filizzola C., Genzano N., Lisi M., Pergola N.; 2015: From Visual Comparison to Robust Satellite Techniques: 30 Years of thermal Infrared Satellite Data Analyses for the Study of Earthquake Preparation Phases. Boll. Geof. Teor. Appl. 56, 167–202.

Zhu F., Su F., Lin J.; 2018: Statistical Analysis of TEC Anomalies Prior to M6.0+ Earthquakes during 2003-2014. Pure Appl. Geophys. 175, 3441–3450.

A comparison between moment magnitude scales

P. Gasperini[1,2], B. Lolli[2]

[1] *Dipartimento di Fisica e Astronomia "Augusto Righi", Università di Bologna, Bologna, Italy*
[2] *Istituto Nazionale di Geofisica e Vulcanologia, Sezione di Bologna, Bologna, Italy*

Moment magnitude M_w was first defined by Kanamori (1977) and Hanks and Kanamori (1979) in the late 1970s, when the availability of new force balance seismometers made it possible to measure the seismic moment M_0 with virtually no limits in the frequency passband. For this reason, M_w does not become saturated even for the largest earthquakes ever recorded. M_w has been chosen in such a way that it coincides best with the previous definitions of magnitude (M_L, m_b, M_s etc.) on certain ranges of values but can deviate significantly from them within other ranges. A few years ago, a new moment magnitude scale M_{wg} was proposed by Das et al. (2019), with the aim of better reproducing the values of m_b and M_s over their entire range and to better predict the energy E_s radiated by earthquakes. In this work we show that there was no need to define such a new scale and that the latter is not even optimal to achieve the goal that the authors had set themselves.

References

Das, R., Sharma, M. L., Wason, H. R., Choudhury, D., and Gonzales. G. (2019). A Seismic Moment Magnitude Scale, Bull Seism. Soc. Am., 109/4, 1542–1555, doi: 10.1785/0120180338.

Kanamori, H. (1977). The energy release in great earthquakes, J. Geophys. Res. 82, 2981–2987.

Hanks, T. C., and H. Kanamori (1979). A moment magnitude scale, J. Geophys. Res. 84, 2348–2350.

Corresponding author: paolo.gasperini@unibo.it

Revealing anomalies in the Molise 2018 earthquake sequence

S. Gentili[1], P. Brondi[1], G. Rossi[1], M. Sugan[1], G. Petrillo[2,3], J. Zhuang[3], S. Campanella[1]

[1] National Institute of Oceanography and Applied Geophysics - OGS, Italy
[2]The Institute of Statistical Mathematics – ISM, Japan;
[3]Scuola Superiore Meridionale – SSM, Italy

Understanding the seismic clustering patterns in a region is crucial for statistical testing and forecasting. The NESTORE (NExt STrOng Related Earthquake – Gentili et al. 2023) algorithm has been shown to be a successful example of such applications of cluster analysis. It can be used for strong aftershock forecasting during an ongoing cluster. However, its forecasting performance can be compromised, if clusters are not properly detected.

With various approaches, including traditional window-based methods, complex network-based techniques, stochastic declustering methods rooted in the Epidemic Type Aftershock Sequence (ETAS) model, and Principal Component Analysis (PCA), this study investigates the seismic sequence in Molise (southern Italy) in 2018. Ambiguous results were obtained when applying the NESTORE method. We utilize an enhanced template matching catalog and four different methods to identify earthquakes belonging to the cluster. While two methods indicate the presence of two distinct clusters in the same area and time period (from April to November 2018), Principal Component Analysis and Nearest Neighbor suggest the presence of a single cluster.

Inconsistencies are attributed to the seismicity potentially being part of anomalous sequences. This research emphasizes the need for refined cluster identification methods and calls for further studies on how to characterize the specific seismic anomaly as in Molise in 2018.

Acknowledgements

Funded by a grant from the Italian Ministry of Foreign Affairs and International Cooperation

References

Gentili, S., P. Brondi, and R. Di Giovambattista; 2023: NESTOREv1.0: A MATLAB Package for Strong Forthcoming Earthquake Forecasting, Seismol. Res. Lett. 94, 2003–2013, doi: 10.1785/0220220327.

Corresponding author: sgentili@ogs.it

Time–Space Evolution of the Groningen Gas Field in Terms of b-Value: Insights and Implications for Seismic Hazard

L. Gulia

Università di Bologna, Bologna, Italia

The Groningen gas field, located in the northeast of The Netherlands, is the Europe's largest onshore gas field. It was discovered in 1959 and production started in 1963: Continuous production has led to reservoir compaction and subsidence, gradual loading of pre-existing faults and induced seismicity that started about 30 yr into the production. The seismic hazard and risk related to the induced seismicity is determined not only for the rate of activity, but it is also equally influenced by the relative size distribution of the seismicity—the b-value. I reanalyze the spatial and temporal evolution of the b-value in the field using an alternative approach to overcome magnitude in completeness heterogeneity, and link it to the evolution of fault loading and subsidence. Spatial variations of b-values are found to vary between 0.61 and 1.3, with the lowest observed values observed in the location of the 2012 M 3.6 Huizinge earthquake. In the last 10 years, the mapped b-values are more homogeneous throughout the field. The spatial and temporal evolution of the b-value in the field in this study is shown to be quite complex, and systematically linked it to the evolution of fault loading, absolute compaction, and the rate of compaction—an important finding that offers new insights into hazard reduction and mitigation strategies of extraction relation-induced seismicity. Compaction rates below 2 mm/yr are not correlated to seismicity above M 2.0 in the history of the field, suggesting that low-volume production may be safer than that previously assumed.

Corresponding author: laura.gulia@unibo.it

The new version of the Foreshock Traffic Light System

L. Gulia[1*], S. Wiemer[2], E. Biondini[1], G. Vannucci[3], B. Enescu[4]

[1] *University of Bologna, Department of Physics and Astronomy, Bologna, Italy*
[2] *Swiss Seismological Service, ETH Zurich, Zurich, Switzerland*
[3]*Istituto Nazionale di Geofisica e Vulcanologia, Bologna, Italy*
[4]*University of Kyoto, Kyoto, Japan*

After the occurrence of a moderate to large earthquake, the question shared between Civil Protection, scientists, the population, and all decision makers is only one: *Was it the mainshock or a bigger event has yet to come?*

According to standard earthquake statistics, the chance that after a moderate earthquake an even larger event will occur within five days and 10 km is typically 5% (Reasenberg and Jones, 1990). Recently, a more specific answer to this question has been given by the Foreshock Traffic Light System (FTLS, Gulia and Wiemer, 2019). The method allows the real-time discrimination between foreshocks and aftershocks in well-monitored regions.

However, some expert judgements are required in order to overcome local peculiarities (Brodsky, 2019) such as magnitude of completeness and the duration of the short-term aftershock incompleteness (STAI; Kagan, 2004).

We here introduce and test the new version of the code that, using the b-positive estimator (van der Elst, 2021), successfully overcomes the above-mentioned limits, allowing the implementation of the FTLS already in few hours after a M≥6 event without any specific expert judgements.

References

Brodsky, E. (2019). Predicting if the worst earthquake has passed. Nature, 574, 185-186.

Gulia, L., and S. Wiemer (2019). Real-time discrimination of earthquake foreshocks and aftershocks, Nature 574, 193–199.

Kagan, Y. Y. (2004). Short-term properties of earthquake catalogs and models of earthquake source. Bull. Seism. Soc. Am., 94(4), 1207–1228. https://doi.org/10.1785/012003098

van der Elst, N. J. (2021). B-positive: A robust estimator of aftershock magnitude distribution in transiently incomplete catalogs. J. Geophys. Res. Solid Earth, 126, e2020JB021027. https://doi.org/10.1029/2020JB021027

Corresponding author: laura.gulia@unibo.it

Fault System Finite-Element Geodynamical Modelling for Seismic Hazard Analysis of the Central Italian Apennines

A. Rood[1], M. Pagani[1], D. Di Bucci[2]

[1]*GEM Foundation, Pavia, Italy*
[2]*Dipartimento della Protezione Civile, Presidenza del Consiglio dei Ministri, Rome, Italy*

The structural complexity of the Italian Apennines, as a result of the sequential overprint of successive tectonic phases, presents a significant challenge in the study of the seismotectonics of the region for earthquake hazard analysis. Specifically, the effect of this structural complexity is that the interpretation of surface geological and geodetic observations may not completely characterise the 3-D distribution of fault geometries and their seismicity in the subsurface. Therefore, to understand the seismotectonics of the Apennines, for the goal of accurate seismic hazard analysis of this seismically active region, it is potentially valuable to characterise the seismogenic potential of faults both at surface and in the subsurface. The structural complexity of the Apennines and its consequences on the seismotectonic setting was recently emphasized by the pattern of seismicity across the Central Apennines during the 2016–2017 seismic sequence (Chiaraluce *et al.*, 2017). The reported fault segmentation, reactivation, and interaction within this fault system demonstrates the need for these phenomena to be taken into account when analysing the seismic hazard for this region (Buttinelli *et al.*, 2021a).

To achieve this goal, we employed the RETRACE-3D model (Buttinelli *et al.*, 2021b) of the fault system that characterises the crustal volume affected by the 2016-2017 seismic sequence (Di Bucci *et al.*, 2021; RETRACE-3D Working Group, 2021) for use in geodynamic modelling using the Geodynamic World Builder (Fraters *et al.*, 2019). We then integrated this model with the finite element code ASPECT (Bangerth *et al.*, 2022; Kronbichler *et al.*, 2012) to determine the instantaneous long-term strain rate of each fault in the fault system. This is a new application of ASPECT to the modelling of active faults systems for seismic hazard analysis. Perhaps not unexpected, we find that major faults take over most of the extension imposed as a boundary condition (Stemberk *et al.*, 2019) and that the interaction between the faults within the fault system is evident from the spatial variability of strain rate over an individual fault surface.

We utilised the OpenQuake engine (Pagani *et al.*, 2014) to then conduct a probabilistic seismic hazard analysis (PSHA) for the region that contains the RETRACE-3D model, using the ASPECT modelling results. The seismic moment rate of each fault was calculated from the total strain rate across the fault surface, which was then used to determine the rate of occurrence of a characteristic, full-fault rupture. Our RETRACE-3D hazard results show a good agreement with the hazard results using the ESHM20 fault model (Danciu *et al.*, 2021) at low probabilities of exceedance. Finally, disaggregation by source allowed the identification of the faults within the fault system that are the main contributors to the hazard for some representative sites. This innovative PSHA model for the Central Italian Apennines represents one of the first applications of geodynamic finite-element modelling of a highly complex fault system to characterise the 3-D distribution of seismic strain within the subsurface for a hazard analysis.

In this contribution, we present preliminary results, recognising that our work to date has revealed plenty of directions for subsequent work to be done. Such future work might include, for example, not only improving the rheology of the various components of the finite-element model but also abandoning the hypothesis of full segmentation. An approach to build a fault-based occurrence model by considering the full set of faults as part of an interconnected system of sections would be similar to the state-of-the-art hazard models in other regions of the world, such as California and New Zealand.

References:

Bangerth, W., Dannberg, J., Fraters, M., Gassmoeller, R., Glerum, A., Heister, T., Myhill, R., & Naliboff, J. (2022). ASPECT: Advanced Solver for Problems in Earth's ConvecTion, User Manual. https://doi.org/10.6084/m9.figshare.4865333.v9

Buttinelli, M., Petracchini, L., Maesano, F. E., D'Ambrogi, C., Scrocca, D., Marino, M., Capotorti, F., Bigi, S., Cavinato, G. P., Mariucci, M. T., Montone, P., & Di Bucci, D. (2021a). The impact of structural complexity, fault segmentation, and reactivation on seismotectonics: Constraints from the upper crust of the 2016–2017 Central Italy seismic sequence area. *Tectonophysics*, *810*, 228861. https://doi.org/10.1016/j.tecto.2021.228861

Buttinelli, M., Maesano, F. E., Petracchini, L., D'Ambrogi, C., Scrocca, D., Di Bucci, D., Basili, R., Cara, P., Castenetto, S., Giuliani, R., Salvi, I., Bigi, S., Cavinato, G. P., Di Filippo, M., Messina, P., Castaldo, R., De Novellis, V., Pepe, S., Solaro, G., . . . Ventura, R. (2021b). *RETRACE-3D Central Italy Geological Model.* Italian Institute for Environmental Protection and Research (ISPRA). https://doi.org/10.13127/RETRACE-3D/GEOMOD.2021

Chiaraluce, L., Di Stefano, R., Tinti, E., Scognamiglio, L., Michele, M., Casarotti, E., Cattaneo, M., De Gori, P., Chiarabba, C., Monachesi, G., Lombardi, A., Valoroso, L., Latorre, D., & Marzorati, S. (2017). The 2016 Central Italy Seismic Sequence: A First Look at the Mainshocks, Aftershocks, and Source Models. *Seismological Research Letters*, *88*(3), 757-771. https://doi.org/10.1785/0220160221

Danciu, L., Nandan, S., Reyes, C., Basili, R., Weatherill, G., Beauval, C., Rovida, A., Vilanova, S., Sesetyan, K., Bard, P.-Y., Cotton, F., Wiemer, S., & Giardini, D. (2021). *The 2020 update of the European Seismic Hazard Model: Model Overview*. https://doi.org/10.12686/a15

Di Bucci, D., Buttinelli, M., D'Ambrogi, C., Scrocca, D., & RETRACE-3D Working Group. (2021). RETRACE-3D project: a multidisciplinary collaboration to build a crustal model for the 2016-2018 central Italy seismic sequence. *Bollettino di Geofisica Teorica ed Applicata*, *62*, 1-18. https://doi.org/doi:10.4430/bgta0343

Fraters, M., Thieulot, C., van den Berg, A., & Spakman, W. (2019). The Geodynamic World Builder: a solution for complex initial conditions in numerical modeling. *Solid Earth*, *10*(5), 1785-1807. https://doi.org/10.5194/se-10-1785-2019

Kronbichler, M., Heister, T., & Bangerth, W. (2012). High accuracy mantle convection simulation through modern numerical methods. *Geophysical Journal International*, *191*(1), 12-29. https://doi.org/10.1111/j.1365-246X.2012.05609.x

Pagani, M., Monelli, D., Weatherill, G., Danciu, L., Crowley, H., Silva, V., Henshaw, P., Butler, L., Nastasi, M., Panzeri, L., Simionato, M., & Vigano, D. (2014). OpenQuake Engine: An Open Hazard (and Risk) Software for the Global Earthquake Model. *Seismological Research Letters*, *85*(3), 692-702. https://doi.org/10.1785/0220130087

RETRACE-3D Working Group. (2021). *RETRACE-3D: centRal italy EarThquakes integRAted Crustal modEl. Final report. eds. INGV, ISPRA, CNR-IGAG, DPC. Rome, p. 100.* https://doi.org/10.5281/zenodo.4604940

Stemberk, J., Moro, G. D., Stemberk, J., Blahůt, J., Coubal, M., Košťák, B., Zambrano, M., & Tondi, E. (2019). Strain monitoring of active faults in the central Apennines (Italy) during the period 2002–2017. *Tectonophysics*, *750*, 22-35. https://doi.org/https://doi.org/10.1016/j.tecto.2018.10.033

Corresponding Author: anna.rood@globalquakemodel.org

Performance of the Ground Motion Models to predict the significant durations in Italy

B. Shoaib[1], F. Ramadan[2], G. Lanzano[2], M. Sadek[3], H. EL Ghoche[3]

[1] *University of Camerino, Italy*
[2] *Istituto Nazionale di Geofisica e Vulcanologia, Italy*
[3] *Lebanese University – Faculty of Technology, Lebanon*

Within the framework of seismic probabilistic hazard analysis and other engineering-oriented applications, the common approach to predict the ground motion is to use ground motion prediction models (GMMs). Those models are empirically developed as a function of a few explanatory variables such as magnitude, source-to-site distance, site condition, and focal mechanism. Traditionally, GMMs are developed for peak ground acceleration (PGA), peak ground velocity (PGV), and the ordinates of the acceleration response spectra (SA); however, to fully describe the dynamic response, other intensity measurements should be considered, such as the Arias intensity and ground motion duration.

The main aim was to study the ground motion durations caused by moderate-to-high earthquakes in Italy and to contribute to the development of a new duration GMM within the Italian context, by analysing the performance of existing GMMs against recordings of recent earthquakes in Italy.

Among several definitions of waveform duration, we considered as a reference intensity measure the relative significant durations (DSR), that are related to Arias Intensity, according to two definitions (Bommer et al., 2009): i) the DSR(5-75) measures the time interval from the 5%up to 75% of the total AI; ii) the DSR(5-95) extends to 95% of the Arias intensity.

An Italian shallow crustal dataset (ITA18) (Lanzano et al., 2022) has been considered, already employed for the GMMs calibration of other strong motion parameters (Lanzano et al. 2019; Ramadan et al. 2021); the dataset presents records for 154 events taken from 1637 stations. The dataset is dominant with events of Mw<5, NF focal mechanism, and site type A and B (According to the EC8 site classification).

Based on the above mentioned definitions, DSR(5-75) and DSR(5-95) were computed for all records found in the dataset ITA18: Husid function (Arias intensity vs time) was estimated for each acceleration waveform to obtain the time frames corresponding at each specific percentage of the total arias intensity (5%, 75%, and 95%).

Figure 1 reports the correlogram of the intensity measures and explanatory variables: it shows the measures of the “strength” of the linear relationship between the DSRs and the variables: a strong positive correlation with RJB and a moderate positive correlation with Mw were observed, as expected. The correlations with the other variables are weaker, probably also due to the uncertainty associated with their estimation.

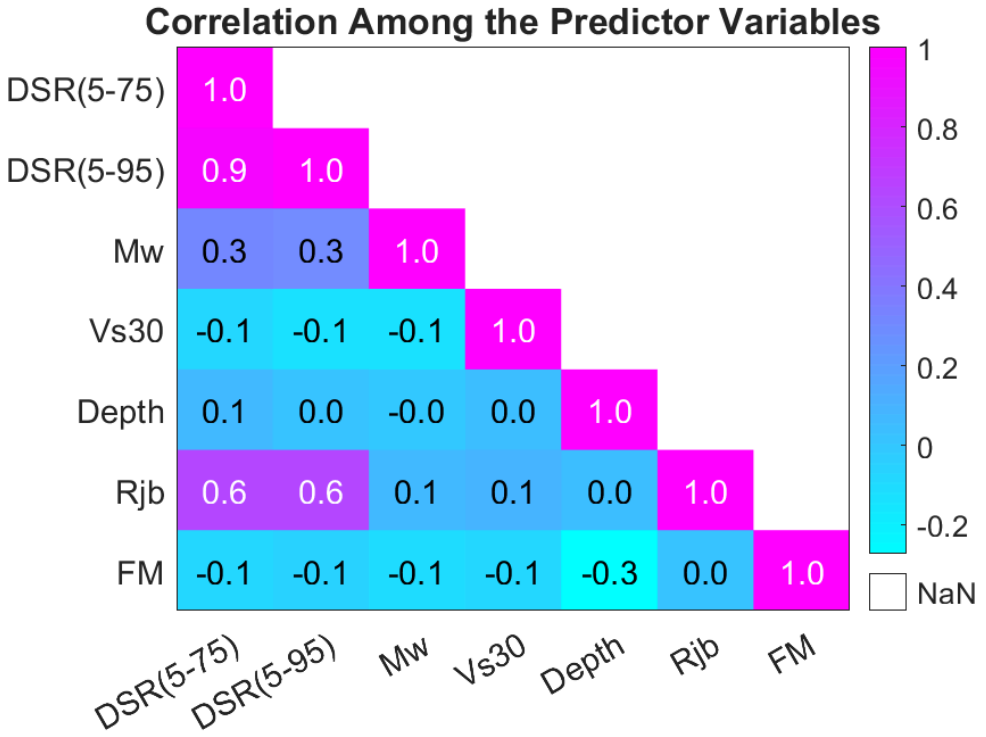

Figure 1: Durations' Correlations for Geometric Mean of the Horizontal Components with GMMs explanatory variables

Residuals were calculated, which represent the difference between the observed durations and the duration predicted by a specific model. It shows how well or poorly a model's predictions are close to the observed duration. After observing the duration, the predicted duration was calculated according to the models given by Bommer et al., (2009), Afshari and Stewart (2016), and Tafreshi and Bora (2023). Bommer et al., (2009) model and study were based on a strong motion dataset extracted from the database compiled for the NGA-West project (Chiou et al., 2008), whose main purpose is to calibrate GMM for active crustal earthquakes in the Western US. The dataset used consists of 2406 records from 114 earthquakes with moment magnitudes in the range from 4.8 to 7.9. Afshari and Stewart (2026) model was based on the NGA-West2 project (Ancheta et al., 2014), and it was reduced to 11,284 duration pairs of duration parameters for two as-recorded horizontal components with a Mw range between 3.0-7.9 events. Tafreshi and Bora (2023) model was calibrated on an Iranian strong motion database. The dataset used consists of 1749 records from 566 events with a Mw range from 3 to 7.5, recorded at 338 stations from 1976 to 2020. The total residual was calculated for each record by subtracting the logarithmic of the observed duration from the logarithmic of the predicted duration. Logarithmic was used since the durations are log-normally distributed. The distribution showed that all the models on average underestimated the observed durations, but the model by Afshari and Stewart (2016) has a better median performance and lower associated variability (Figure 2).

These results suggest that the functional form proposed by Afshari & Stewart (2016) is a good starting point for the calibration of a new predictive model for duration in Italy.

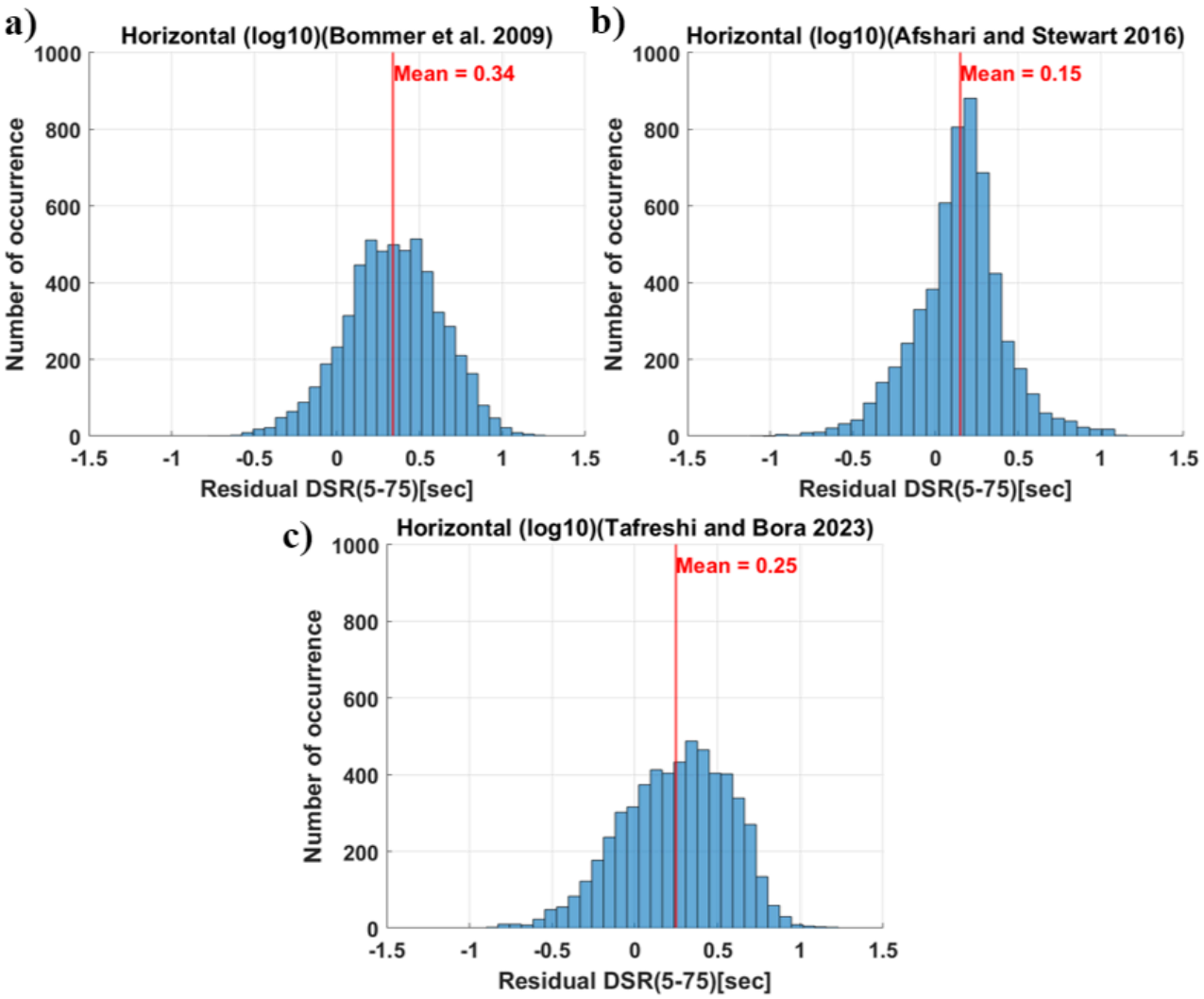

Figure 2: Residual for the horizontal DSR(5-75) for the Three Models: a) Bommer et al. 2009, b) Afshari and Stewart 2016, and c) Tafreshi and Bora 2023

The residuals were subsequently decomposed by applying the random effects approach (Al Atik et al. 2010) into offset (a0), between event (δBe), site-to-site (δS2Ss), and event-and-site corrected (δW0es) terms to check that the scaling with magnitude, distance, and V_{S30} (which are the main explanatory variables) of the considered models are compatible with those observed for ITA18. The results showed that all the models did not capture the magnitude scaling of ITA18 data: Bommer et al. (2009) and Tafreshi and Bora (2023) have similar trends, underestimating the low magnitude durations and overestimating the high magnitude ones. Afshari & Stewart (2016) GMM has a better median performance, but the duration observed for high magnitude earthquakes are underestimated (Figure 3-a,d & g). The other residuals did not exhibit significant bias, except for the event and site corrected residuals of Tafreshi and Bora (2023), which showed a different scaling with distance, probably because the model mimics the regional attenuation characteristics of Iran, for which the model was calibrated.

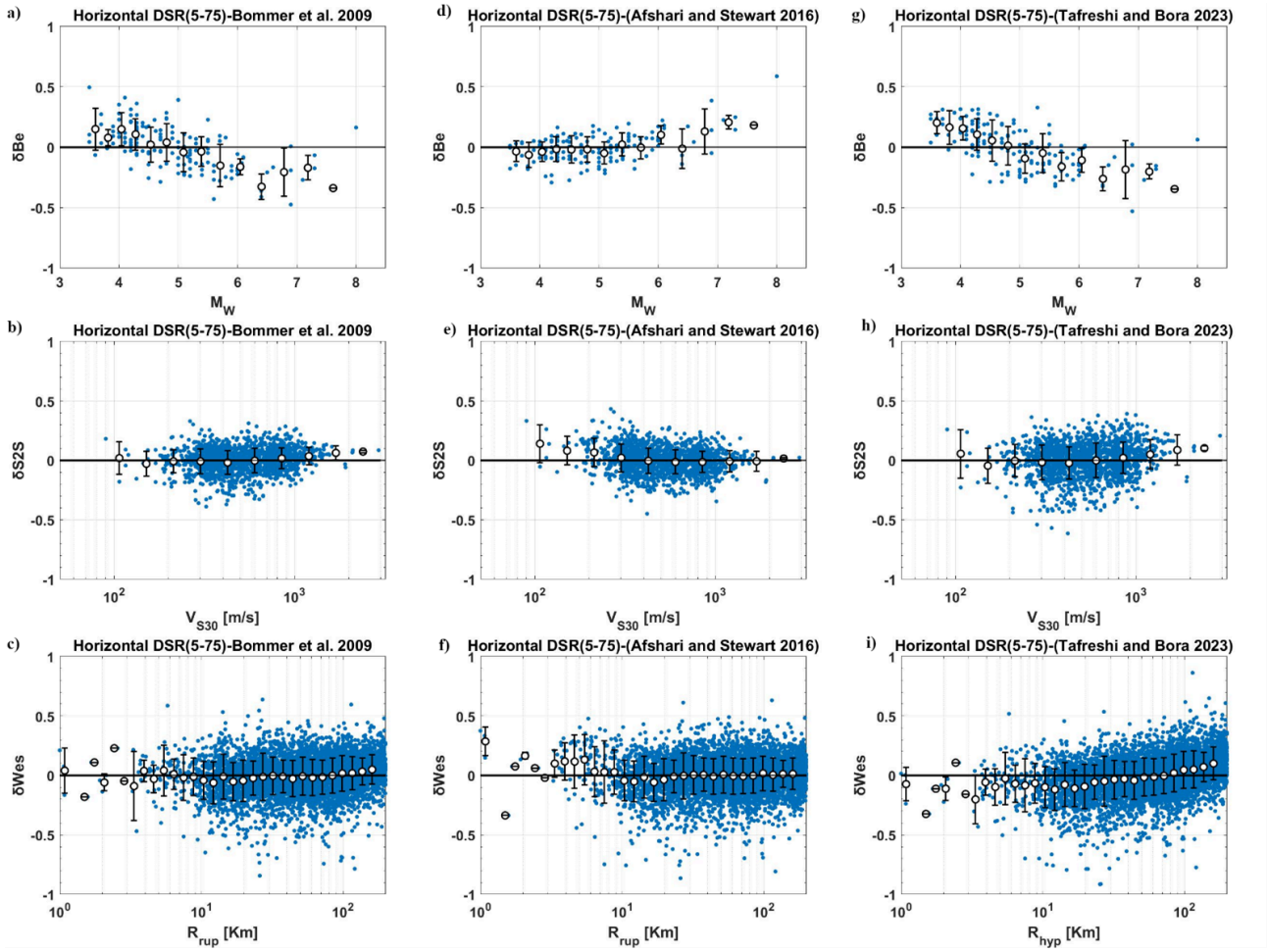

Figure 3: Distribution of a) between events residuals for Bommer, et al., (2009) model, b) site-to-site residuals for Bommer, et al., (2009) model, c) event-and-site residuals for Bommer, et al., (2009) model, d) between events residuals for Afshari & Stewart, (2016) model, e) site-to-site residuals for Afshari & Stewart, (2016) model, f) event-and site residuals for Afshari & Stewart, (2016) model, g) between events residuals for Tafreshi and Bora (2023) model, h) site-to-site residuals for Tafreshi and Bora (2023) model, i) event-and-site residuals for Tafreshi and Bora (2023) model.

References

Afshari K., and Stewart J. P.; (2016): Physically Parameterized Prediction Equations for Significant Duration in Active Crustal Regions. Earthquake Spectra, 29.

Al Atik L., Abragamson N., Bommer JJ., Scherbaum F., Cotton F., Kuehn N., The variability of ground-motion prediction models and its components. Seismol Res Lett. 2010;81(5):794-801.

Ancheta T. D., Darragh R. B., Stewart J. P., Seyhan E., Silva W. J., Chiou B. S.-J., Wooddell K. E., et al.; (2014): NGA-West2 Database. Earthquake Spectra, 30, 989–1005.

Bommer J. J., Stafford P. J., and Alarcón, J. E.; (2009): Empirical Equations for the Prediction of the Significant, Bracketed, and Uniform Duration of Earthquake Ground Motion. Bulletin of the Seismological Society of America, 99(6), 3233.

Chiou B., Darragh R., Gregor N., and Silva W.; (2008): NGA Project Strong-Motion Database. Earthquake Spectra, 24(1), 23–44.

Lanzano G., Luzi L., Pacor F., et al.; (2019): A revised ground-motion prediction model for shallow crustal earthquake in Italy. Bull Seismol Soc Am.; 109(2):525-540.

Lanzano G., Ramadan F., Luzi L., Sgobba S., Felicetta C., Pacor F., D'Amico M.C., Puglia R., Russo E.; (2022): Parametric table of the ITA18 GMM for PGA, PGV and Spectral Acceleration ordinates. Istituto Nazionale di Geofisica e Vulcanologia (INGV). <https://doi.org/10.13127/ita18/sa_flatfile>

Ramadan F., Smerzini C., Lanzano G., Pakor F.;(2021): An empirical model for the vertical-to-horizontal spectral ratios for Italy. Earthquake Engineering and structural dynamics; 50(15): 3937-4219.

Tafreshi M. D., and Bora S. S.; (2023): Empirical ground motion models (GMMs) and associated correlations for cumulative absolute velocity, Arias intensity, and significant durations calibrated on Iranian strong motion database. Bulletin of Earthquake Engineering, 21, 4139–4166.

Corresponding author: batoul.a.shoaib@gmail.com

The database of the Catalogue of Strong Earthquakes in Italy and in the Mediterranean Area (CFTI): exploring historical seismology through modern web tools

G. Tarabusi[1], C. Ciuccarelli[1], M.G. Bianchi[1], C. Zei[1,2], D. Mariotti[1], G. Sgattoni[1], R.C. Taccone[1], G. De Francesco[1], G. Ferrari[1], G. Valensise[1], CFTI working group

[1] *Istituto Nazionale di Geofisica e Vulcanologia, Italy*
[2] *Dept. of Physics and Earth Sciences, Ferrara University, Italy*

CFTI, the Catalogue of Strong Earthquakes in Italy and in the Mediterranean Area, is an analytical inventory that stores in a large database the results of four decades of research in Historical Seismology on Italy and on the Mediterranean area.

CFTI is both parametric and analytical, as for most of the analysed earthquakes it features descriptive summaries of both the effects of each specific event at each individual location, and of its overall social and economic impact. But it is also a fully transparent database, as for each investigated earthquake sequence it provides a complete bibliography of all available testimonies of scholars and casual observers: many of such testimonies are supplied on-line, either in the form of the original source or as a transcription.

Since the beginning of the research in 1983, the Working Group developed a specific computerised cataloguing scheme of all historical materials identified along selected research paths. The work was extremely extensive from its very beginning; numerous previously unknown or poorly known earthquakes were added to the previously available wealth of knowledge. The method used for unearthing and organising the new information and the resulting elaborations has been gradually refined and consolidated in the subsequent versions of the CFTI.

The current version of the catalogue, termed CFTI5Med (Guidoboni et al., 2018; Guidoboni et al., 2019), includes 1,167 earthquakes for the Italian area and 473 earthquakes for the extended Mediterranean region (the latter section deals exclusively with ancient and medieval events). It hence draws from an extremely valuable and unique documentary and historical heritage: one of the most important in the world, in terms of quantity, quality and geographic distribution of the available information, and also in terms of the relevant chronological interval, spanning over two millennia (from the 8th century B.C. to the 15th century for Mediterranean area; from the 5th century B.C. to the 20th century for Italy).

Since the release of CFTI5Med, which features an entirely renovated and advanced web interface, we added various datasets and developed new IT tools, all accessible via the CFTILab web portal (Tarabusi et al., 2020), which are the result of synergistic collaboration among the various skills that exist in the CFTI Working Group. Our aim was to enable multiple specialist and non-specialist users – including scholars, civil protection officers, teachers, students, professionals, and simply curious citizens – to explore and analyse efficiently the extensive wealth of data stored in the Catalogue. We briefly present here four of its main components (tools and datasets).

CFTIcompare is a web-based tool that allows for a visual comparison of the effects of two different earthquakes, or of the intensity data supplied by two different studies of the same earthquake.

The comparison is performed on a geographical basis, and may concern either data from the CFTI alone (which are shown along with summaries of the effects for each individual location) – for example to compare the effects of two earthquakes that occurred in adjacent areas – or from other databases (e.g. ASMI, DBMI, Hai sentito il terremoto?).

The user may also use his/her own dataset, provided that it is organised following one of the three allowed input formats.

CFTIvisual (Bianchi et al., 2022) is the Atlas of visual sources on Italian historical earthquakes (Fig. 1).

About four decades of investigation of Italian historical earthquakes led to the retrieval of many visual sources, including engravings, paintings, photographs, film documents, etc. They may be useful to scholars from different disciplines for supplementing information on the estimation of damage, on the response of institutions, on scientific observations, etc.

Currently the Atlas allows for advanced consultation of all visual sources that concern Italian earthquakes and can be freely published. Dedicated links allow connecting the sources to contextual descriptive information from CFTI.

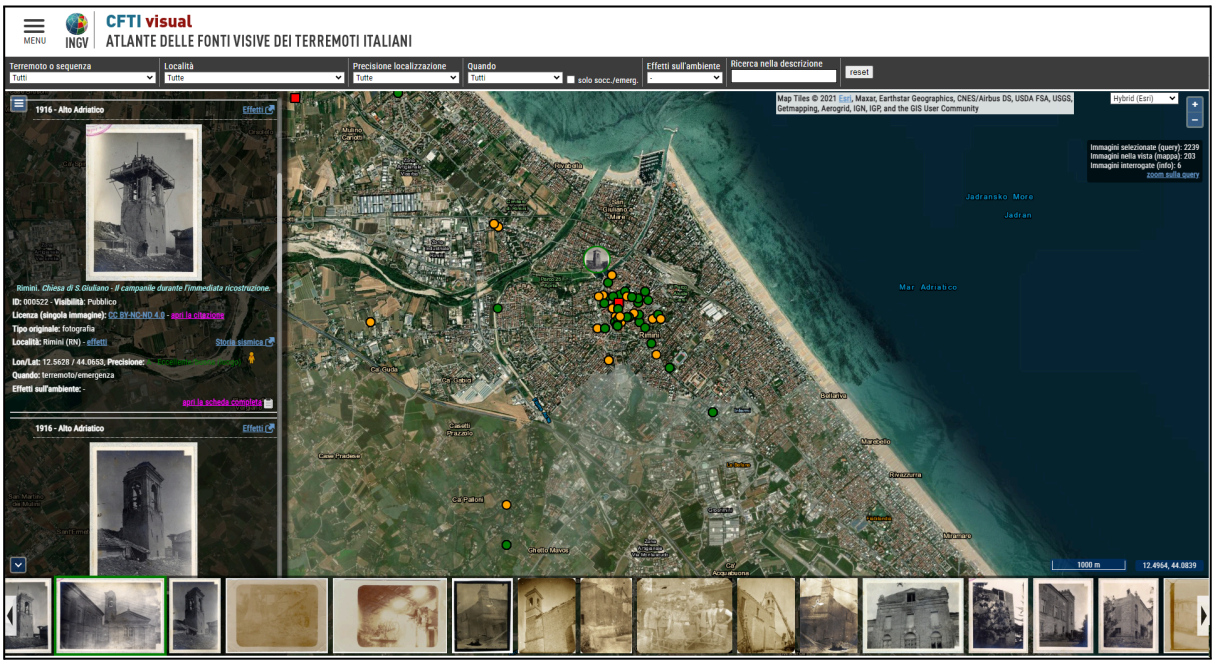

Fig. 1 - CFTIvisual web interface.

CFTIsequences displays the earthquake sequences through interactive graphs and maps (Fig. 2). This result has been made possible through extensive data review of historical sources aimed at integrating and validating data related to the chronology, the location, and the effects of individual shocks.

It allows users to consult the available data for individual shocks and for individual locations while keeping all descriptive textual comments visible.

Since the publication of its first release (1995), the CFTI paid much attention to the existence of any foreshocks and aftershocks and of their time and space evolution. This was accomplished by dedicating a specific descriptive commentary to these shocks.

This product is fully functional: it currently contains two sequences for demonstration purposes only, but will soon provide data from more than 100 sequences stored in the CFTI.

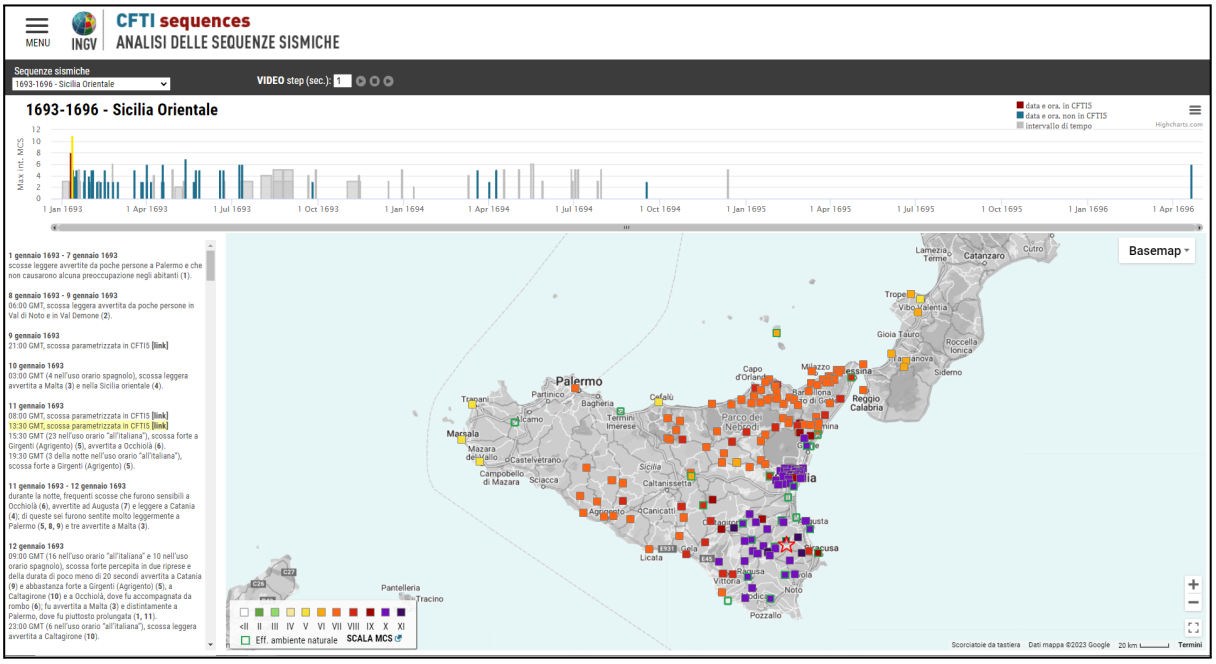

Fig. 2 - CFTIsequences web interface.

CFTIlandslides (Zei et al., 2023) is the Italian database of historical earthquake-induced landslides (Fig. 2).

The investigation of earthquake-induced environmental phenomena is becoming increasingly critical for civil protection agencies. In particular, earthquake-triggered landslides may cause significant losses and may delay rescue operations across large areas.

The combination of a relatively frequent seismic release with a very high landslide susceptibility makes the Italian territory especially prone to the occurrence of earthquake-induced landslides.

This is a new dataset that was developed starting from the effects on the natural environment stored in CFTI5Med. It features over 1,200 landslides, subdivided into classes based on location accuracy and type of movement. It is addressed to a large audience of potential users, including researchers and scholars, administrators and technicians belonging to local institutions, civil protection authorities.

A single, comprehensive web portal is currently under development to provide access to all these products.

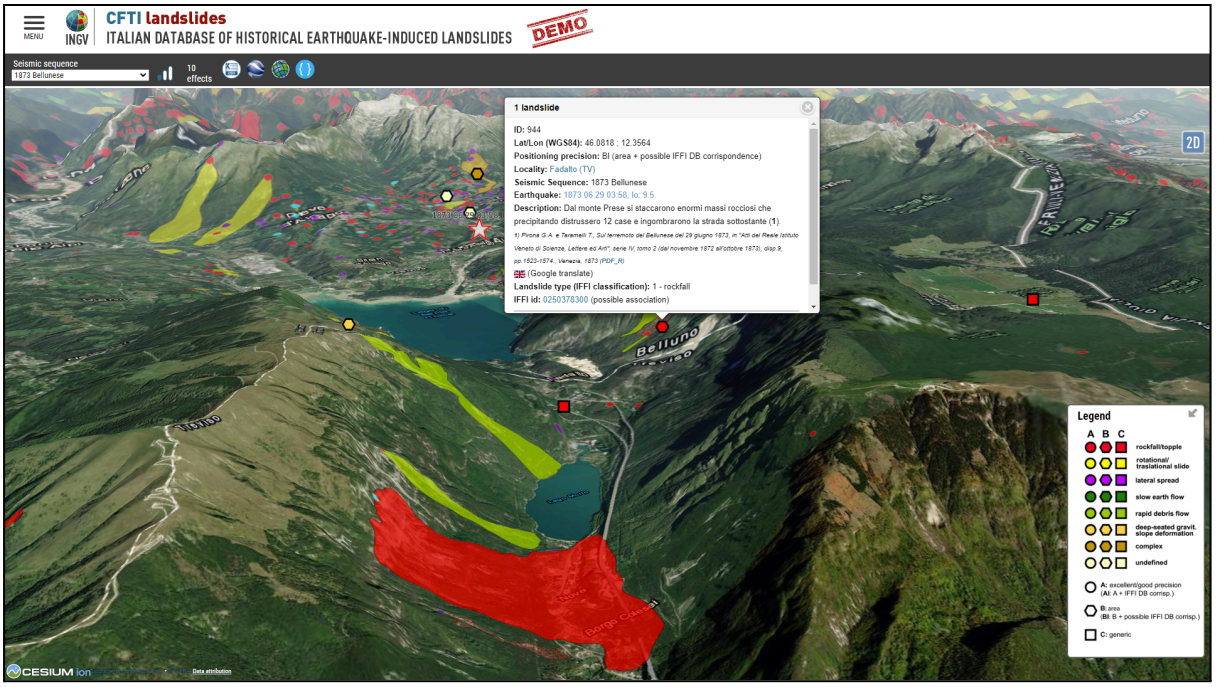

Fig. 3 - CFTIlandslides web interface (3D Map View).

Acknowledgments

Part of the activities have been supported by a grant from Italy's Presidenza del Consiglio dei Ministri-Dipartimento della Protezione Civile. Nevertheless, the views and conclusions reported are the sole responsibility of the authors, and should not be interpreted as necessarily representing official policies, either expressed or implied, of the Dipartimento della Protezione Civile.

References

Bianchi M.G., Tarabusi G., Ciuccarelli C., Maresci M., Baranello S., Taccone R.C., Ferrari G., 2022. CFTIvisual, Atlante delle fonti visive dei terremoti italiani. Istituto Nazionale di Geofisica e Vulcanologia (INGV). https://doi.org/10.13127/cfti/visual

Guidoboni E., Ferrari G., Mariotti D., Comastri A., Tarabusi G., Sgattoni G., Valensise G., 2018. CFTI5Med, Catalogo dei Forti Terremoti in Italia (461 a.C.-1997) e nell'area Mediterranea (760 a.C.-1500). Istituto Nazionale di Geofisica e Vulcanologia (INGV). doi: https://doi.org/10.6092/ingv.it-cfti5

Guidoboni E., Ferrari G., Tarabusi G., Sgattoni G., Comastri A., Mariotti D., Ciuccarelli C., Bianchi M.G., Valensise G., 2019, CFTI5Med, the new release of the catalogue of strong earthquakes in Italy and in the Mediterranean area, Scientific Data 6, 80. doi: https://doi.org/10.1038/s41597-019-0091-9

Tarabusi G., Ferrari G., Ciuccarelli C., Bianchi M.G., Sgattoni G., Comastri A., Mariotti D., Valensise G., Guidoboni E. , 2020, CFTILab, Laboratorio Avanzato di Sismologia Storica. Istituto Nazionale di Geofisica e Vulcanologia (INGV). https://doi.org/10.13127/CFTI/CFTILAB

Zei C., Tarabusi G., Ciuccarelli C., Mariotti D., Baranello S., Sgattoni G., Burrato P., CFTI working Group; 2023: *A new database of historical earthquake-induced landslides in Italy*, 41st National Conference of the GNGTS, Bologna https://gngts.ogs.it/atti/GNGTS2023/HTML/212/

Corresponding author: gabriele.tarabusi@ingv.it

The estimation of b-value of the frequency-magnitude distribution and of its one-sigma intervals from binned magnitude data

S. Tinti[1], P. Gasperini[1,2]

[1] *Dipartimento di Fisica e Astronomia "Augusto Righi", Università di Bologna, Bologna, Italy*
[2] *Istituto Nazionale di Geofisica e Vulcanologia, Sezione di Bologna, Bologna, Italy*

The estimation of the slope (b-value) of the frequency magnitude distribution of earthquakes is based on a formula derived by Aki (1965) decades ago, assuming a continuous exponential distribution. However, as the magnitude is usually provided with a limited resolution, its distribution is not continuous but discrete. In the literature this problem was initially solved by an empirical correction (due to Utsu, 1966) to the minimum magnitude, and later by providing an exact formula such as that by Tinti and Mulargia 1987, based on the geometric distribution theory. A recent paper by van der Elst (2021) showed that the b-value can be estimated also by considering the magnitude differences (which are proven to follow an exponential discrete Laplace distribution) and that in this case the estimator is more resilient to the incompleteness of the magnitude dataset.

In this work we provide the complete theoretical formulation including i) the derivation of the means and standard deviations of the discrete exponential and Laplace distributions; ii) the estimators of the decay parameter of the discrete exponential and trimmed Laplace distributions; and iii) the corresponding formulas for the parameter b. We further deduce iv) the standard one-sigma intervals for the estimated b. Moreover, we are able v) to quantify the error associated with the Utsu (1966) minimum-magnitude correction.

We tested extensively such formulas on simulated synthetic datasets including complete catalogues as well as catalogues affected by a strong incompleteness degree such as aftershock sequences where the incompleteness is made to vary from one event to the next.

References

Aki, M. (1965). Maximum likelihood estimate of b in the formula log N = a – bM and its confidence limits, Bull. Earthquake Res. Inst., Tokyo Univ. 43, 237-239. https://doi.org/10.15083/0000033631.

Tinti, S. & Mulargia, F. (1987). Confidence intervals of b values for grouped magnitudes. Bull. Seism. Soc. Am., 77, 2125-2134. Doi: 10.1785/BSSA0770062125.

Utsu, T. (1966). A statistical significance test of the difference in b-value between two earthquake groups, J. Phys. Earth 14, 34–37. https://doi.org/10.4294/jpe1952.14.37.

van der Elst, N. J. (2021). B-positive: A robust estimator of aftershock magnitude distribution in transiently incomplete catalogs. J.of Geophys. Res.: Solid Earth, 126, e2020JB021027. https://doi. org/10.1029/2020JB021027.

Corresponding author: paolo.gasperini@unibo.it

The Multi Synthetic Catalog Analysis (MSCA) as a tool to evaluate seismic hazard, risk and resilience

T. Tufaro[1]

[1] *School of Civil Engineering, University of Basilicata, I-85100 Potenza, Basilicata, Italy*

The classical approach to seismic hazard evaluation is the PSHA method (Cornell, 1968). It is still an excellent approach if we are interested in computing seismic hazard only. However if we wish to include other quantities such as risk or resilience it is better to follow a different method.

The proposal presented here is based on the concept of building a very large number of synthetic catalogs (up to several hundred thousands) that will result in tens of millions of events. It naturally allows for inclusion of:

Risk and resilience scenarios probability;

Time evolution.

The acceleration is computed at each site and the damage is evaluated: each event generates a complete probabilistic scenario. Let us suppose focusing on bridges; a damage scenario where fragility curves can be considered also probabilistic, will lead to the possibility of computing the total repairing cost and necessary timing. This in turn will allow for evaluating the disturbance to local communities, the interruption of local traffic and the overall time necessary to recover it. All of the aboves can be evaluated with a probabilistic setting. The statistics are then conducted on all scenarios. The underlying idea is that, set the quantity we are looking for, let us say the numbers of days commuters loose because of road interruption, and set the number of synthetic catalogs, let us say 100.000, we will select the 100.000 largest values (out of even tenths of millions of events) where the 10% probability threshold will be the one at the 90.000 largest value. Every scenario has a centroid, so the process can be repeated for every possible centroid location. It is obviously a very computationally heavy approach but it can give the appropriate view where major issues are expected. Moreover it is possible to introduce a full time dependent seismic evaluation of the hazard. Fig.1 shows the hazard due the classical seismic zoning (attenuation: Bindi et al., 2011). Since the attenuation law is different from those used in the MPS04, it looks obviously slightly different but it conveys the idea of the equivalence of the two approaches.

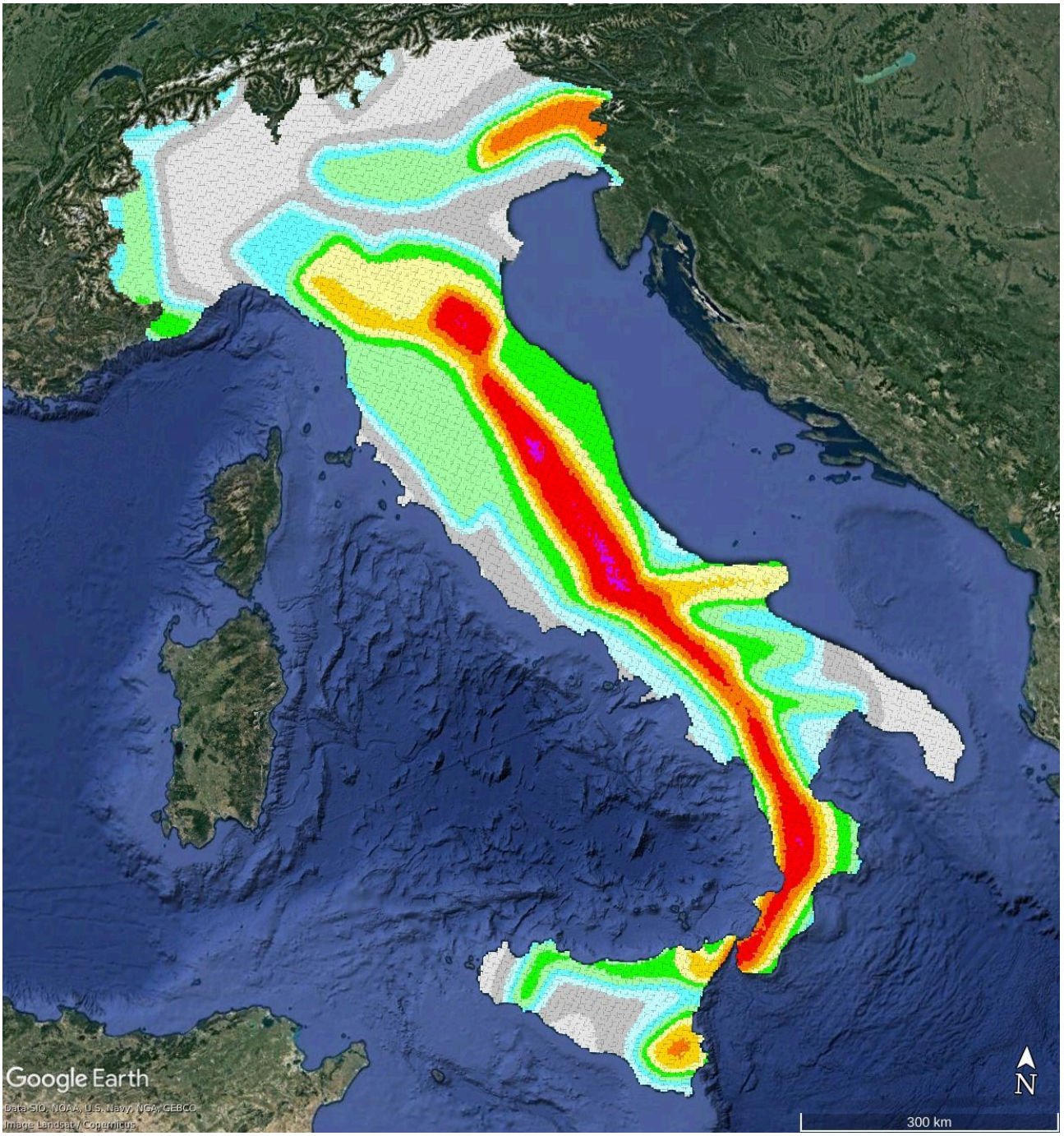

Fig.1 Hazard map due to classical seismic zoning (attenuation: Bindi et al., 2011).

To give a flavour of what the proposed method can achieve, Fig.2 shows the results of a prototypical non poissonian approach where the 10% exceeding probability is not in 50 years but in the next 50 years.

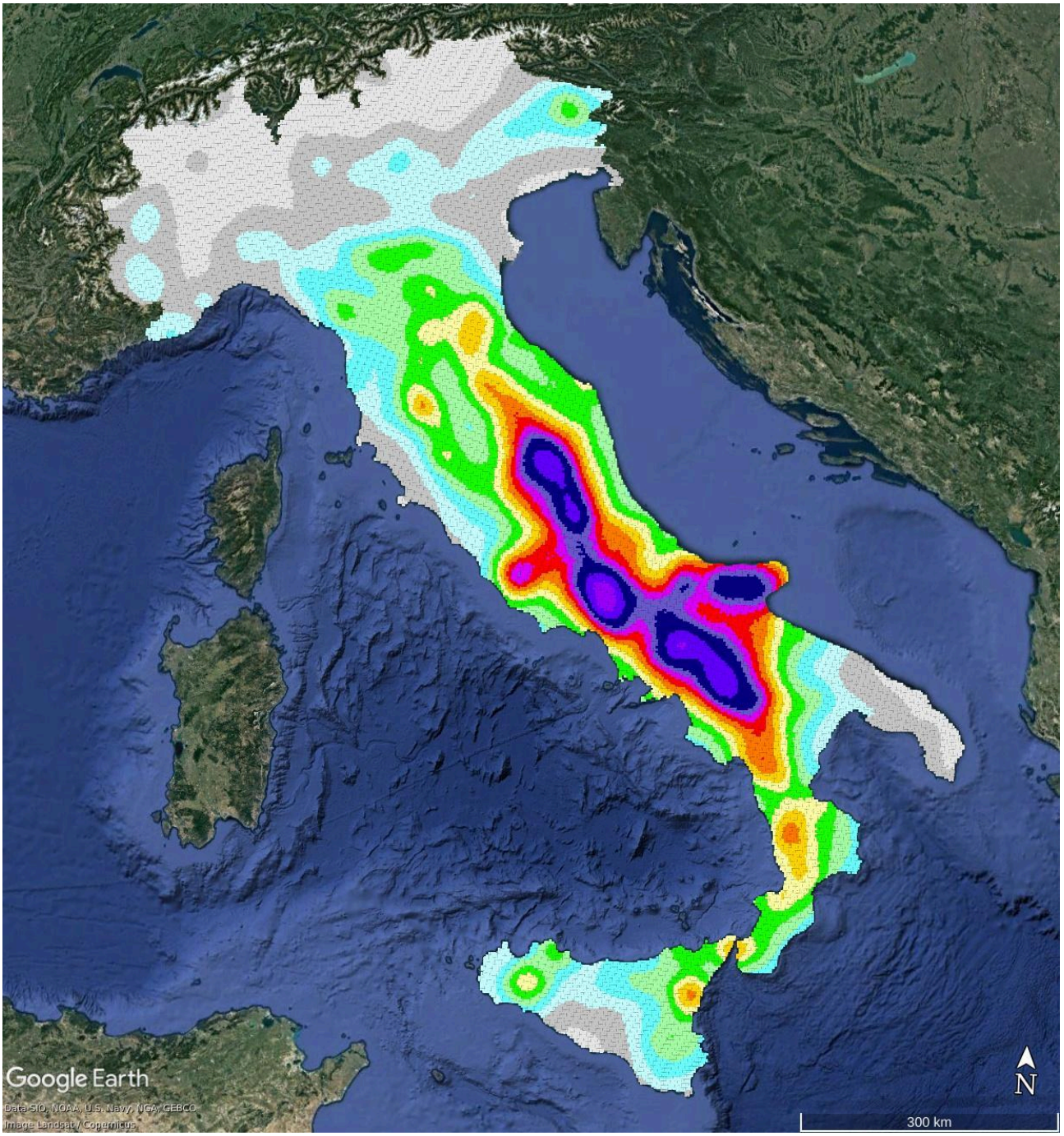

Fig.2 Thematic map of the results obtained through a prototype non-Poissonian approach in which the probability of exceeding 10% is not in 50 years but in the next 50 years.

This model was kindly given by the group (based in University of Basilicata, OGS, INGV-OV, and University of Trieste) that is developing it, and it is based on an extension of Harabaglia (2020) approach. It is based on earthquake data (HORUS) of Lolli et al., (2020) with magnitude M>3.95 in the time interval 1960-2022, and it takes into account the historical locations of the CPTI15 catalog (Rovida et al., 2022) in the time interval 1000-1959. It must be no means be intended as an actual proposal of earthquake hazard in the next 50 years, since the model must still be tuned, but only as an example of what the MSCA can do.

References

Bindi D., Pacor F., Luzi L., Puglia R., Massa M., Ameri G., Paolucci R.; 2011: Ground motion prediction equations derived from the Italian strong motion database. Bull Earthquake Eng, 9(6), 1899–1920. doi:10.1007/s10518 -011-9313.

Cornell; C.A. 1968: Engineering seismic risk analysis. Bull. Seismol. Soc. Am 58, 1583-1606.

Harabaglia P.; 2020: Non-Poissonian Earthquake Occurrence Probability through Empirical Survival Functions Appl. Sci. 2020, 10(3), 838; https://doi.org/10.3390/app10030838 Submission received: 13 December 2019 / Revised: 15 January 2020 / Accepted: 18 January 2020 / Published: 24 January 2020

Lolli B., Randazzo D., Vannucci G., Gasperini P.; 2020: The Homogenized Instrumental Seismic Catalog (HORUS) of Italy from 1960 to Present, Seismol. Res. Lett, doi: 10.1785/0220200148.

Rovida A., Locati M., Camassi R., Lolli B., Gasperini P., Antonucci A.; 2022: Catalogo Parametrico dei Terremoti Italiani (CPTI15), versione 4.0. Istituto Nazionale di Geofisica e Vulcanologia (INGV). https://doi.org/10.13127/CPTI/CPTI15.4.

Corresponding author: ttufaro250@gmail.com

Un confronto teorico tra scale macrosismiche utilizzate in Italia

G. Vannucci[1], B. Lolli[1], P. Gasperini[2,1]

[1]Istituto Nazionale di Geofisica e Vulcanologia, Sezione di Bologna, Bologna, Italy
[2]Dipartimento di Fisica e Astronomia "Augusto Righi", Università di Bologna, Bologna, Italy

In un recente lavoro (Vannucci et al., 2021) abbiamo evidenziato alcune discrepanze empiriche tra le stime dell'intensità macrosismica in Italia nell'ultimo decennio rispetto ai precedenti periodi. Una possibile ragione potrebbe essere la progressiva adozione da parte dei ricercatori italiani della Scala Macrosismica Europea (EMS, Grünthal et al., 1998) al posto della scala Mercalli Cancani Sieberg (MCS; Sieberg, 1912, 1932) utilizzata invece in maniera prevalente fino al 2009. In teoria, in un insediamento moderno in cui gli edifici in cemento armato (RC) stanno sempre più sostituendo quelli in muratura, l'intensità EMS dovrebbe sovrastimare quella MCS perché la prima tiene conto della minore vulnerabilità degli edifici in RC, mentre la seconda non menziona affatto gli edifici in RC poiché questi erano quasi assenti all'epoca in cui fu compilata. Tuttavia, tale deduzione teorica è contraddetta dall'evidenza empirica che, in media, le intensità MCS realmente stimate in Italia nell'ultimo decennio sovrastimano leggermente la EMS e non viceversa come dovrebbe essere. Una possibile spiegazione è che la scala EMS non sia stata ben calibrata per riprodurre la MCS come era nelle intenzioni dei suoi autori. Un'altra possibile ragione delle discrepanze tra l'ultimo decennio e i precedenti potrebbe essere che la scala MCS applicata oggi non è la stessa definita da Sieberg all'inizio del XX secolo. Per comprendere meglio le possibili cause di queste discrepanze, presentiamo qui un confronto formale tra le definizioni dei diversi gradi di tali scale macrosismiche.

References

Grünthal, G. (Editor) (1998). European Macroseismic Scale 1998, Vol. 13, Conseil de l'Europe, Cahiers du Centre Européen de Géodynamique et de Séismologie, Luxembourg, Luxembourg, 99 pp.

Sieberg, A. (1912). Über die makroseismische Bestimmung der Erdbebenstärke. Ein Beitrag zur seismologische Praxis, G. Gerlands Beitr. Geophys. 11, nos. 2/4, 227–239 (in tedesco).

Sieberg, A. (1932). Erdebeben, in Handbuch der Geophysik, B. Gutenberg (Editor), Vol. 4, 552–554 (in tedesco).

Vannucci G, Lolli B, Gasperini P (2021) Inhomogeneity of macroseismic intensities in Italy and consequences for macroseismic magnitude estimation. Seism Res Lett 92:2234–2244. Doi: 10. 1785/0220200273.

Corresponding author: gianfranco.vannucci@ingv.it

Do not call them foreshocks

D. Zaccagnino[1*], L. Telesca[2], C. Doglioni[1,3]

[1] *Sapienza University, Earth Sciences Department, Rome, Italy*
[2] *Institute of Methodologies for Environmental Analysis, National Research Council, Tito, Italy*
[3] *Istituto Nazionale di Geofisica e Vulcanologia (INGV), Rome, Italy*

One of the most intriguing issues in earthquake science concerns the discrimination between foreshocks and swarms. We investigate relocated seismic catalogues in California and Italy and provide a theoretical explanation of our results.

Foreshocks and swarms share the same scaling behaviours and are likely generated by the same physical mechanism; however, statistical analyses highlight that foreshocks spread over larger areas, are featured by larger and more energetic clusters with also higher variance of magnitudes and relative Tsallis and Shannon entropies. On the other hand, foreshocks have duration, seismic rates, and moment rates, as well as magnitude trends and clustering properties indistinguishable from swarms. Our results prove that mainshocks can occur with or without foreshocks with extremely variable magnitudes. In fact, in crustal volumes, the value of stress at a certain time depends on the history of recently happened variations of the stress itself, depending on memory kernels, and fine-scale structural details of fault interfaces and tectonic forces. This means that even two identical seismic clusters can flow into a large mainshock, moderate events or a swarm depending on the action of tiny details in the evolution of stress gradients. On the other hand, two completely different seismic patterns can give rise to seismic events with similar features. This result strongly challenges the possibility of accurate earthquake prediction, both in terms of time to failure and magnitude, at least just considering past seismic activity. A mathematical model is realized to explain our observations.

Clusters covering large areas are displays of long-range correlations within larger crustal volumes. As tectonic strain increases the level of stress, faults become more and more unstable, until a spontaneous rupture develops on the weakest interface. Static and dynamic stress variations trigger further events afterwards within the crustal volume showing significant correlations with the hypocenter, i.e., sensitivity to stress perturbations. The larger the region close to instability, the more seismic events can be triggered and with statistically higher magnitudes. This is the reason why mainshocks tend to happen after clusters spread over larger areas, with higher number of events and magnitudes not because such seismic activity ultimately triggers them. However, foreshocks are not “fore-shocks''; they are not informative about the magnitude or time-to-failure of the eventually impending earthquake. Earthquakes ultimately grow to become giant events because of fine details of differential stress patterns and

fault strength, regardless of previous seismic activity, if the extension of the prone-to-failure volumes is large enough.

References

Shannon C.E. (1948). A mathematical theory of communication. Bell Syst. Tech. J., **27**(3), 379-423.

Tsallis C. (1988). Possible generalization of Boltzmann-Gibbs statistics. J. Stat. Phys., **52**, 479-487.

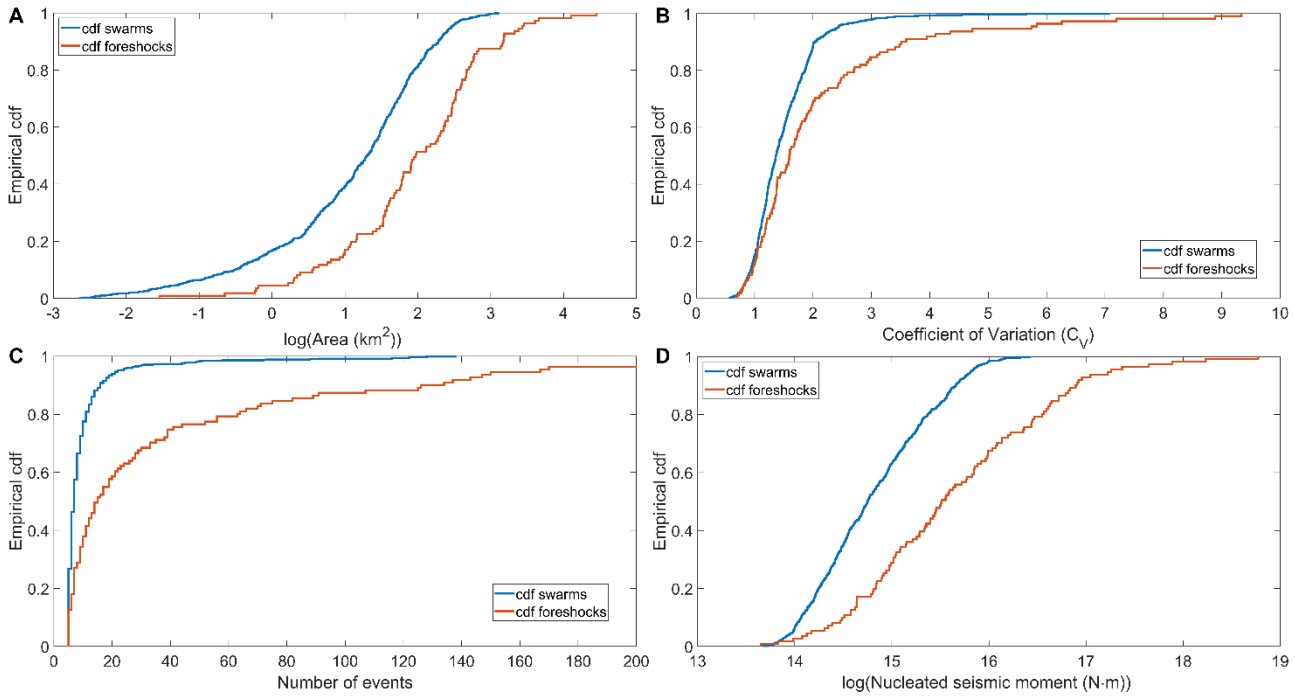

Fig. 1: Cumulative distribution of the number of seismic events in each cluster until the mainshock as a function of their various features: area (A), global coefficient of variation (B), number of events (C), nucleated seismic moment (D) in Southern California from 1981 to 2022 (only events with Mw > 2.5 are included in the analysis).

Possible applications of self-similarity in earthquake clustering to seismic hazard

D. Zaccagnino[1*], L. Telesca[2], C. Doglioni[1,3]

1 Sapienza University, Earth Sciences Department, Rome, Italy

2 *Institute of Methodologies for Environmental Analysis, National Research Council, Tito, Italy*
3 Istituto Nazionale di Geofisica e Vulcanologia (INGV), Rome, Italy

We perform an analysis to understand what information may be hidden in partial, limited earthquake catalogues only containing mid-size and a few large seismic events (or even no one) about the largest possible ones using clustering properties of recorded events. We consider the local and global coefficients of variation, the scaling exponent of the Gutenberg–Richter law, the fractal dimension of epicentral series D_f, the seismic rate and the number of events. We find that the largest earthquakes occur in locally Poissonian systems (local coefficient of variation of interevents L_V 1) with globally clustered dynamics (global coefficient of variation C_V1). While local clustering in time is strongly dependent on the size of the catalogue, so that longer databases tend to be less regular and more Poissonian than shorter ones, the global coefficient seems to be a reliable parameter even in cases of rather limited available information, e.g., few thousand events (Zaccagnino et al., 2023a). We analyse regional seismicity in different tectonic settings getting analogous results, e.g., Southern California, Cascadia (Zaccagnino et al., 2022), Italian Apennines, New Zealand (Zaccagnino et al., 2023a), and Turkey (Zaccagnino et al., 2023b). The fractal dimension of spatial series is positively correlated with the seismic rate, C_V and the maximum listed magnitude. Conversely, the b-value does not show any correlation with the principal observables except for the number of earthquakes. We explain this phenomenon considering the different sizes of mainshocks in various tectonic settings. We propose that the predictive power of clustering properties stems from the self-similar nature of slow dynamics producing the emergence of slips in complex systems such as the brittle crust. Prospectively, this approach can be of great interest, once tuned, to extrapolate the features of extreme, still unobserved events given a limited database.

References

Zaccagnino D., Telesca L. and Doglioni C.; 2022: Variable seismic responsiveness to stress perturbations along the shallow section of subduction zones: The role of different slip modes and implications for the stability of fault segments. Front. Earth Sci., 10, 989697.

Zaccagnino D., Telesca L. and Doglioni, C.; 2023: Global versus local clustering of seismicity: Implications with earthquake prediction. Chaos Solit. Fractals, 170, 113419.

Zaccagnino D., Telesca L., Tan O. and Doglioni, C.; 2023: Clustering Analysis of Seismicity in the Anatolian Region with Implications for Seismic Hazard. Entropy, 25(6), 835.

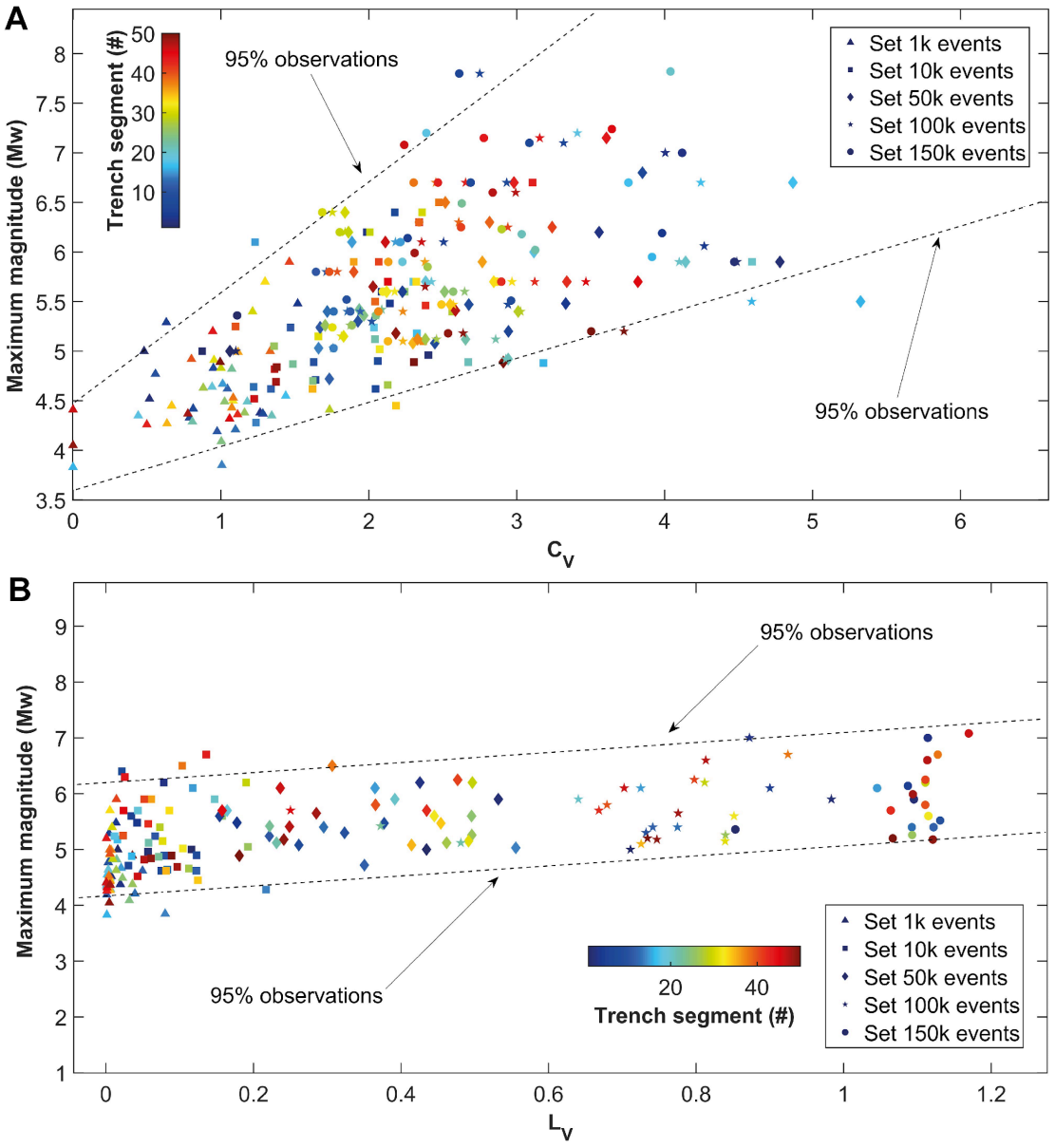

Fig. 1 (A) Maximum observed magnitude in catalogue vs global coefficient of variation for fifty segments of seismogenic sources in New Zealand (represented by the colour) calculated using different portions of the seismic catalogue (Mw>Mc, depth < 50 km, 1985-2022), i.e., < 1%, ~ 7%, ~ 1/3, ~ 2/3 and full catalogue, one of each kind, in chronological order. This situation simulates how clustering properties of seismicity change with time as the amount of recording increases. Extremely short catalogues (corresponding to few months of recordings) are almost Poissonian with low maximum magnitude, while mid-length and long catalogues showcase clustered seismicity. The behaviour of seismic activity in the latter cases seems to be long-term time invariant, i.e., the degree of global clustering increases almost linearly. Therefore, regions with higher CV fixed the size of the catalogue may be prone to larger earthquakes. (B) Maximum observed magnitude in catalogue vs local coefficient of variation. While extremely short catalogues are locally periodic, mid-length and long catalogues showcase locally-Poissonian seismicity. Only slight positive correlation is observed between maximum magnitude and the local coefficient of variation.

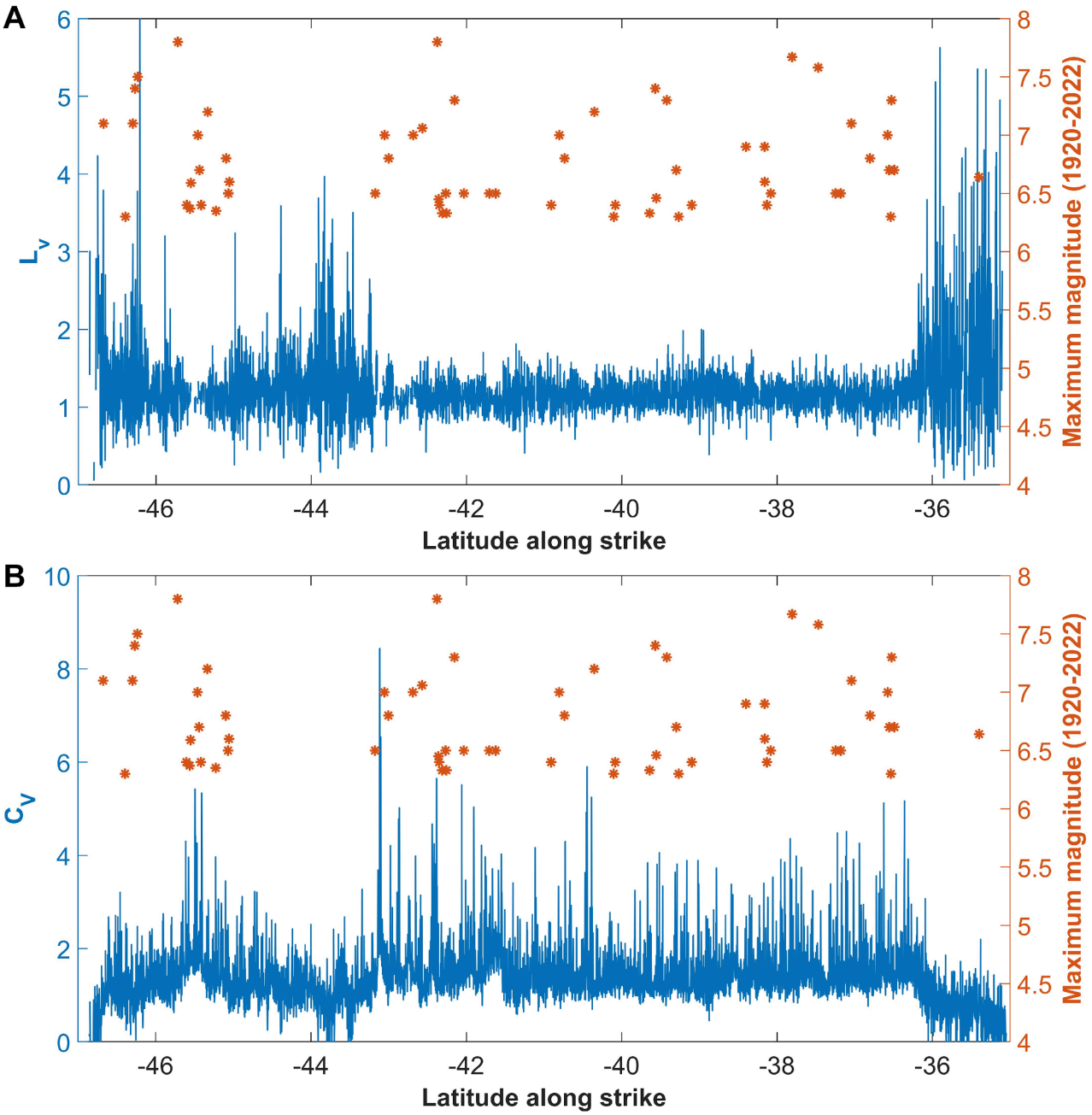

Fig. 2: Coefficients of variation for seismicity along the most important seismogenic structures in New Zealand between 1985 and 2022. (A) Local coefficient of variation and maximum observed magnitudes from 1920 and 2022 above Mw 6.0. Large seismic events tend to occur where seismic activity is locally Poissonian. (B) Global coefficient of variation and maximum historical magnitudes from 1920 and 2022. Large seismic events tend to occur where seismicity is globally clustered.